ANALYZING THE EFFICIENCY OF THE COLORIMETRIC TECHNIQUE IN DETERMINING THE DEGREE OF HEMOLYSIS OF STORED BLOOD

by

Osman Melih Can

BS, in Biomedical Engineering

Yeditepe University, 2010

Submitted to the Institute of Biomedical Engineering

in partial fulfillment of the requirements

for the degree of

Master of Science

in

Biomedical Engineering

Boğaziçi University

2014

ANALYZING THE EFFICIENCY OF THE COLORIMETRIC TECHNIQUE IN DETERMINING THE DEGREE OF HEMOLYSIS OF STORED BLOOD

APPROVED BY:

Prof. Dr. Yekta Ülgen (Thesis Advisor)	.....
Prof. Dr. Ata Akın	.....
Assoc. Prof. Dr. Murat Gülsoy	.....

DATE OF APPROVAL: 8 January 2014

ACKNOWLEDGMENTS

First of all, I would like to express my graditute to my thesis supervisors Prof. Dr. Ata Akın and Prof. Dr. Yekta Ülgen for their academic support and guidance with endless patience throughtout my graduate study. I also thank Asst. Prof Dr. Bora Garipcan and Asst. Prof. Dr. Özgür Kocatürk due to their valuable suggestions and feedback through my graduate study and Assoc. Prof. Dr. Murat Gülsoy, member of my thesis committee for his valueable support during my thesis defense.

I would like to thank Dr. Hülya Bilgen, Director of Transfusion Center in Florence Nightingale Hospital for sharing their facilities everytime I need.

I am very thankful to Recep Murtazaoğlu, İsmail Devecioğlu, Alparslan Bilir, Fırat Şansal, Murat Tümer, Yunus Engin Gökdağ and Selçuk Kandemir for their willingness to blood donation for the study.

I am very grateful to my dear wife Sevil Can for her love and assistance to experiments at weekends and some nights. I am very much thankful to my family; Ahmet, Cemile and Mithat Can for thier endless support with patience. I thank so much my grandmother and grandfather Gülsen and İbrahim Köse and I wish to thank my grandmother Hüsniye Can who always wanted to see my best days.

ABSTRACT

ANALYZING THE EFFICIENCY OF THE COLORIMETRIC TECHNIQUE IN DETERMINING THE DEGREE OF HEMOLYSIS OF STORED BLOOD

Transfusion has risks of adverse outcomes on patients due to the storage lesions of blood products. Measuring quality of the blood prior to usage can minimize the transfusion related reactions. For controlling the quality of units, experts visually assess the degree of hemolysis by comparing color of blood with graded color charts. Since results are subjective and depend on the spectral energy distribution of the illuminant, the method is inaccurate. Instead of using color charts, color of the stored blood can quantitatively be measured by analyzing the spectrum of the light reflected from the sample with a spectrometer. The color of blood can be defined as a set of tristimulus values or color coordinates in the color space. In this study daily changes in the colorimetric parameters of stored blood were monitored and correlated with the changes in the degree of hemolysis. Red blood cell (RBC) suspensions collected from 7 male volunteers were used for the study. On each day of storage, 24 colorimetric parameters in various color spaces were measured with a reflection probe that transmits both the incident light from the light source to the blood bag; and the reflected light from the blood bag to the spectrometer. Standard hemolysis measurements with Harboe technique were performed on weekly basis, by taking blood samples from blood bags. Colorimetric parameters: tristimulus X, u', u-v saturation, Hunter a, CIE a*, CIELAB chroma and the correlated color temperature (CCT) changed significantly ($p<0.05$) for each sample after the 3^{rd} week of storage. Except CCT, hemolysis showed good correlation ($r>0.65$) with the parameters that mostly correspond to red contents of the color stimuli. Hunter a apparently is the most suitable parameter for determining the degree of hemolysis with ($r=0.71$) ($p<0.005$).

Keywords: Red Blood Cell Storage, Hemolysis, Storage Lesions, Colorimetry, XYZ color space.

ÖZET

DEPOLANAN KANIN HEMOLİZ DERECESİNİN TAYİNİNDE RENK ÖLÇÜM TEKNİĞİ ETKİNLİĞİNİN ANALİZİ

Kan ürünlerinin depolama lezyonlarından dolayı transfüzyonun hastada kötü sonuçlar doğurma riski bulunur. Uygulamadan önce kanın kalitesini ölçmek transfüzyonla ilişkili reaksiyonları en aza indirebilir. Kan ürünlerinin kalitesini kontrol etmek için, uzmanlar, kanın rengini derecelendirilmiş renk kartlarıyla karşılaştırarak hemoliz derecesini görsel olarak tayin ediyorlar. Bu method hatalıdır, çünkü sonuçlar subjektiftir ve aydınlatıcının spektral enerji dağılımına bağlıdır. Renk kartları kullanmak yerine, depolanmış kanın rengi bir spektrometre ile, örnekten yansıyan ışığın spektrumu analiz edilerek sayısal olarak ölçülebilir. Kanın rengi bir renk uzayında bir takım tristimülüs değerler veya koordinatlarla tanımlanabilir. Bu çalışmada depolanmış kanın renk parametrelerindeki değişimleri günlük olarak izlendi ve hemoliz derecesindeki değişimlerle ilişkilendirildi. Çalışma için 7 erkek gönüllüden alınmış kırmızı kan hücresi süspansiyonları kullanıldı. Depolanan her günde, farklı renk uzaylarındaki 24 renk parametreleri; hem ışığı ışık kaynağından örneğe ileten, hem de örnekten yansıyan ışığı spektrometreye ileten yansıtıcı prob ile ölçüldü. Harboe tekniği ile standard hemoliz ölçümü haftalık olarak, torbadan kan örnekleri alınarak uygulandı. Renk parametreleri: X, u', u-v doygunluğu, Hunter a, CIE a*, CIELAB renk parlaklığı ve renk sıcaklığı, her bir örnek için, 3. haftadan sonra anlamlı ($p<0.05$) şekilde değişti. Renk sıcaklığı hariç, hemoliz; renk uyaranının çoğunlukla kırmızı bileşenlerine karşılık gelen renk parametreleriyle iyi korelasyon ($r>0.65$) gösterdi. Görünen o ki, hemoliz derecesini tayin etmede kullanılabilecek en uygun parametre ($r=0.71$) ($p<0.005$) ile Hunter a'dır.

Anahtar Sözcükler: Hemoliz, Transfüzyon, Kırmızı kan hücreleri, Renk ölçümü.

TABLE OF CONTENTS

LIST OF FIGURES

LIST OF TABLES

LIST OF SYMBOLS

a	Axis of Hunter Lab space
a*	Axis of CIE L*a*b* space
b	Axis of Hunter Lab space
b*	Axis of CIE L*a*b* space
K_m	Constant 683 lmW^{-1}
L	Luminance
L	Axis of Hunter Lab space
L*	Axis of CIE L*a*b* space
P_n	Power at n^{th} wavelength
S_E	Equi-energy stimulus
u	Tristimulus value of CIE 1960 Yuv space
u_0	Coordinate of white point in uv chromaticity diagram
u'	Coordinate of u'v' chromaticity diagram
u'_0	Coordinate of white point in u'v' chromaticity diagram
v	Tristimulus value of CIE 1960 Yuv space
v_0	Coordinate of white point in uv chromaticity diagram
v'	Coordinate of u'v' chromaticity diagram
v'_0	Coordinate of white point in u'v' chromaticity diagram
W'	Tristimulus value of CIE 1964 U'V'W' space
x	Coordinate of xy chromaticity diagram
$\overline{x}(\lambda)$	Color matching function of standard colorimetric observer
X	Tristimulus value of CIE 1931 XYZ system
X_0	Tristimulus value of white point in CIE 1931 XYZ system
V_n	Relative power of luminous efficiency function at n^{th} wavelength
y	Coordinate of xy chromaticity diagram
$\overline{y}(\lambda)$	Color matching function of standard colorimetric observer
Y	Tristimulus value of CIE 1931 XYZ system
Y_0	Tristimulus value of white point in CIE 1931 XYZ system

z	Dependent parameter to x and y coordinates
$\overline{z}(\lambda)$	Color matching function of standard colorimetric observer
Z	Tristimulus value of CIE 1931 XYZ system
Z_0	Tristimulus value of white point in CIE 1931 XYZ system
β	A type of cone most sensitive to blue light
γ	A type of cone most sensitive to green light
λ	Wavelength
ρ	A type of cone most sensitive to red light

LIST OF ABBREVIATIONS

ABO	Blood grouping system
ATP	Adenosine triphosphate
B	Blue
CCT	Correlated color temperature
CIE	Commision Internationale de l'Eclairage
CIELAB	CIE 1976 color space
CPDA	Citrate-phosphate-dextrose-adenine
DAMP	Danger-associated molecular pattern molecules
DPG	Diphosphogylcerate
EAS	Experimental additive solution
FDA	Food and Drug Administration
FNHTR	Febrile non-hemolytic transfusion reactions
G	Green
GVHD	Graft versus host disease
Hb	Hemoglobin
HBV	Hepatitis B virus
HCV	Hepatitis C virus
HIV	Human immunodeficiency virus
HLTV	Human T-lymphotropic virus
MCHC	Mean cell hemoglobin concentration
MOF	Multi organ failure
NADH	Nicotinamide adenine ninucleotide-hydrogen
NO	Nitric oxide
PAGGSM	Phosphate-adenine-glucose-guanosinesaline and mannitol
PAMP	Pathogen-associated molecular pattern molecules
PRT	Pathogen reduction technology
PS	Phosphatidylserine
PTFE	Polytetraflouroethylene

PVC	Polyvinylchloride
R	Red
RBC	Red blood cell
Rejuvesol	Rejuvenating solution
RPH	Reflection probe holder
SAGM	Saline-adenine-glucose-mannitol
SNO-Hb	S-nitrosothiol-hemoglobin
TACO	Transfusion-associated circulatory overload
TRALI	Transfusion-associated lung injury
TRIM	Transfusion-related immunomodulation
V	Violet
W	White
WBC	White blood cell
WS	White standard

1. INTRODUCTION

Red blood cells are the most commonly transfused blood product. Donated blood is stored in blood banks according to approved conditions. Naturally, red cells metabolize throughout storage, so biochemical and mechanical properties of red cells deteriorate progressively. Those changes have been impugned as the cause of numerous adverse clinical effects including multi organ failure (MOF), increased length of stay in the intensive care unit or hospital and mortality especially, for the patients having cardiac problems, microcirculation problems [1]. Best way to minimize transfusion related complications is controlling the quality of each blood products prior to usage [2]. Developing such a non-invasive technique that measures some physiological parameters of RBCs and gives an opportunity to the experts for assessing the quality of the blood would be an important improvement in transfusion medicine.

Currently, before release from blood collection facilities or before transfusion, RBC units are visually inspected for hemolysis which is an important quality indicator [3]. Hemolysis is the breakdown of RBC membrane and releasing of hemoglobin and heme into the plasma. The US Food and Drug Administration (FDA) has recommended a maximum of 1% hemolysis at the end of the storage period. In contrast, the official guideline in Europe adjusted 0.8% as end of storage hemolysis [4]. Hemolysis is usually recognized by the presence of pink discoloration in the suspending media (Figure 1.1). Experts visually assess the degree of hemolysis by the change in red color of the blood. However, estimation of hemolysis by visual inspection is subjective, even with the use of a visual comparator (Munsell, Ostwald system) (see Chapter 3.2), and lacks adequate standardization making inter-laboratory comparison difficult [5], because results depend on the spectral distribution of the illuminant. Therefore, visual estimation of blood color is an inaccurate method for hemolysis assessment [6].

Instead of using color charts, objective color measurement can be performed by using spectrometer. Color of the samples can be numerically described by analyzing

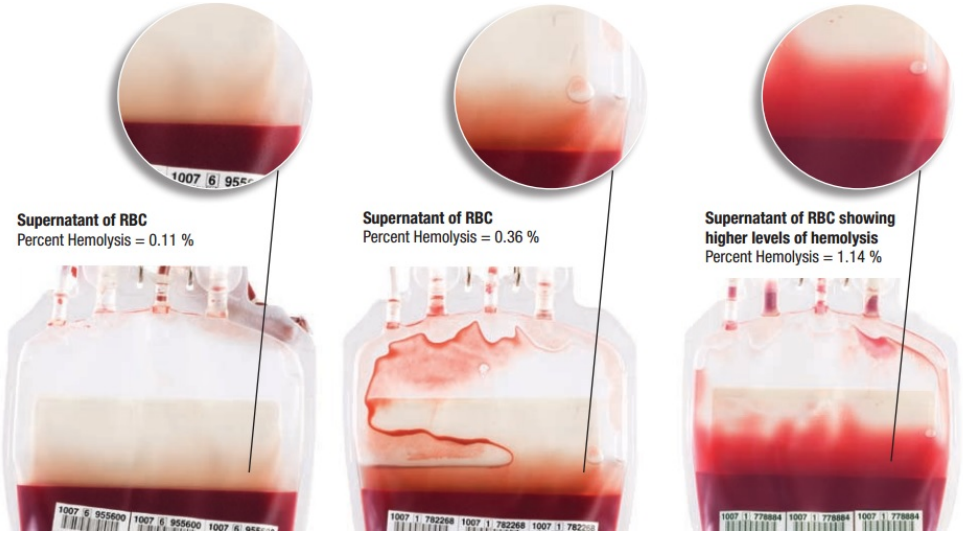

Figure 1.1 Visual assessment of hemolysis from the color change in suspending media. Sample on the right hand side can not be used in transfusion due to higher hemolysis index (>0.8%) [7].

spectrum of light reflected from the surface of the sample. Therefore any relative spectral energy distribution coming from sample to spectrometer can be specified by a set of tristimulus values, or color coordinates in a color space. These tristimulus values and color coordinates, termed as colorimetric parameters, may have relation with hemolysis. The motivation of this study is to monitor daily change in the colorimetric parameters of stored blood and relate them with the change in degree of hemolysis which is measured by the standard Harboe technique.

Although, color change in specially cell free media indicates plasma hemoglobin concentration and degree of hemolysis, there were investigations of hemolysis from whole blood with reflectance measurements [8, 9]. For example, Bermakai *et al.* investigated the hemolysis in whole blood using visible spectrum and studied the factors that affect the patterns of light absorption and transmission caused due to the hemolysis [10]. Similarly, in this study, colorimetric parameters were measured without centrifugation; from outside of the blood bag by using a reflection probe connected both to a spectrometer and a light source.

The aim of this study is to investigate the changes in colorimetric parameters of RBCs in various color spaces during storage, and analyze the correlation between

the colorimetric parameters and degree of hemolysis so as to develop a non-invasive colorimetric technique that measures quality of RBCs by their degree of hemolysis.

Background of the study is expressed in following two chapters. RBC storage is introduced in detail by 4 sections in Chapter 2. Detailed pathology of storage lesions, clinical implications of storage lesions, currently used solutions for minimizing the transfusion related adverse effects and previous studies in developing a quality estimation technique for storage lesions are explained. Then, the science of color, the concept of colorimetry, color vision, various color spaces, color coordinates, tristumulus values are described in Chapter 3.

2. RED BLOOD CELL STORAGE

Transfusion is a life-saving treatment for patients suffering severe blood loss or anaemia due to trauma injury, surgery or other various clinical situations [11]. Approximately, 1.5 million units of whole blood are donated each year in Turkey [12]. Majority of bloods are stored as RBC concentrates in blood banks [13, 14]. After collection of whole blood into polyvinylchloride (PVC) plastic bag which contains anticoagulant solution CPDA (citrate-phosphate-dextrose-adenine), RBCs are prepared by removal of plasma. RBCs are stored in 4 ± 2 ^{o}C in an additive solution, generally SAGM (saline, adenine, glucose, mannitol) which allows storage for 42 days [15]. Although type of additive solution may extend the storage time, Turkish Kızılay and European Council suggests 42 days as a limit of storage [16, 17]. During storage RBCs undergo a variety of physicochemical alterations. These alterations are referred as storage lesions.

2.1 Storage Lesions

RBC storage lesions include metabolic effects, shape change, membrane loss, rheological changes, changes in oxygen affinity and delivery, increased adhesion of RBCs to endothelial cells, increased aggregability, reduced RBC viability, accumulating of some ion concentrations in intra- or extracellular media and bacterial contaminants [18].

RBC metabolism slows at 4 ^{o}C ten times than at 25 ^{o}C. Required energy for RBCs to live inside bag is provided by glycolysis. In glycolysis, glucose is broken down to make adenosine triphosphate (ATP) and lactic acid, carbonic acid and protons are produced as a result. The accumulating protons, lactic acid and carbonic acid make the medium more acidotic, so pH decreases. In addition to low temperature slowing glycolysis, decreasing pH inhibits phosphofructokinase, hexose, kinase (glycolysis enzymes) so that less ATP is made as storage progresses. NADH, the other product of glycolysis

also decreases [19]. Reduced pH also leads to degradation of 2,3-diphosphogylcerate (2,3-DPG). 2,3-DPG is a metabolite and allosteric modifier of hemoglobin which plays a critical role in hemoglobin oxygen affinity regulation. After falling below a pH level of about 7.2 the RBC enzyme 2,3-DPG phosphatase is activated, 2,3-DPG is dephosphorylated to 3-PG and the concentration of 2,3-DPG decreases. Levels of 2,3-DPG falls quickly during storage, becoming undetectable within 2 weeks [20, 21]. During 2,3-DPG dephosphorylation, an initial burst of ATP production occurs. ATP concentration initially rises for 2-3 weeks, stays above their initial value, and then declines steadily [19]. Besides, ATP-dependent major membrane Na-K pumps are inactivated due to the low temperature and ATP level [15]. After 3 days of storage, potassium leaks slowly out of RBCs and sodium accumulates within cytoplasm. The concentration of extracellular potassium increase progressively with a rate of about 1 mEq/L per day [18, 22] and can reach 50 mEq/L [23].

Sequence of shape changes is observed during the second and third week mostly due to acidification, decreasing ATP and oxidative damage of membrane proteins and lipids. Depletion of ATP increases the level of intracellular calcium, protein dephosphorylation and membrane kinases which maintain membrane integrity. Forming of asymmetry in phosphorylation mechanism in erythrocyte leads to increase in phosphatidylinositol-4-phosphate which is accompanied by appearence of echinocytes from normal deformable biconcave disc shape. Subsequently echinocytes swell to form a crenated sphere with multiple long spicules called a spheroechinocyte (Figure 2.1) [24]. At day 7, 9.5% of red blood cells forms echinocytes, spheroechinocytes or spherocytes [25]. In parallel with these changes, redistribution and loss of phospholipids in RBC membrane, oxidative stress resulting in lipid peroxidation and oxidation of transmembrane proteins, cytoskeletal proteins contribute to the formation of microvesicles and membrane changes [26, 27].

Shape changes and membrane defects of RBCs are associated with rheologic changes such as increase in osmotic fragility, aggregability, intracellular viscosity with the loss of surface to volume ratio and the increasing of mean cell hemoglobin concentration (MCHC); and decrease in deformability [24].

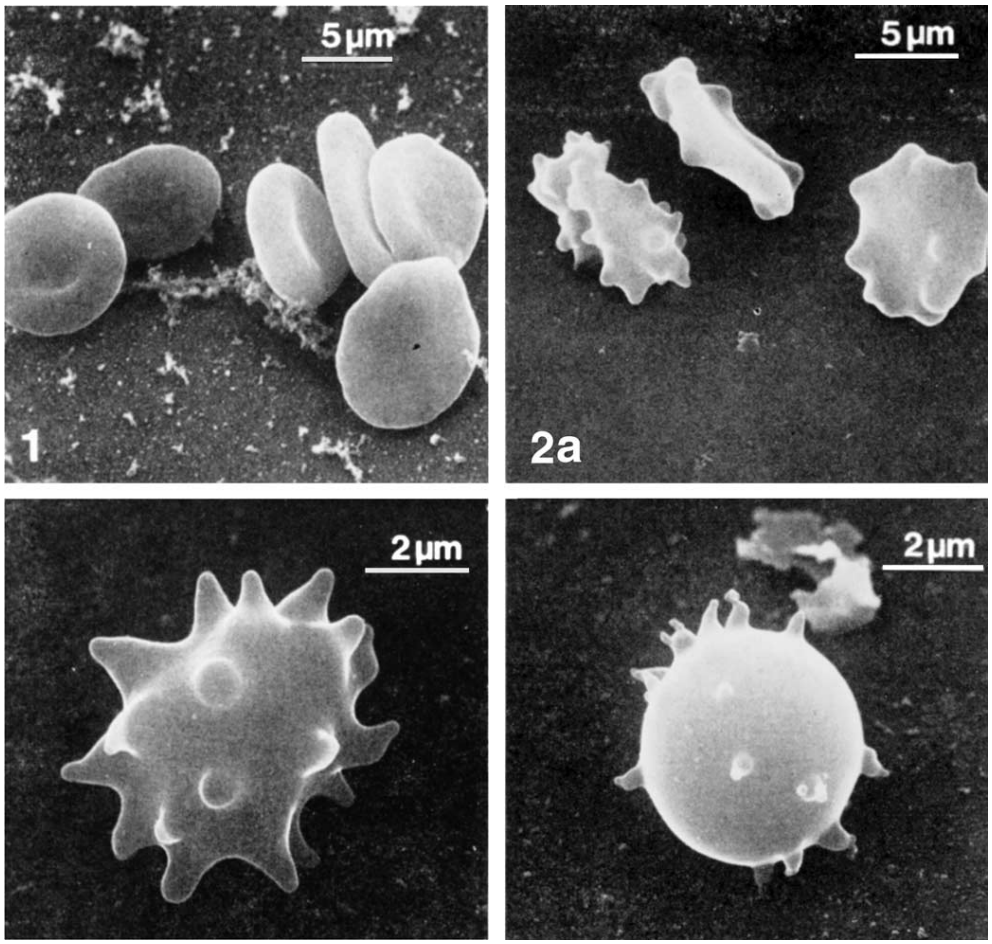

Figure 2.1 Morphological changes of RBCs during storage. Normal RBCs with discoid shape (top left) turn into echinocytes (top right, bottom left) and spheroechinocytes (bottom right) in the following weeks of storage [28].

RBC membrane defects, decreasing deformability and osmotic fragility and pH changes play a role in storage-induced hemolysis [4]. Hemolysis represents the breakdown or disruption of integrity of RBC membranes with the release of hemoglobin directly into the suspending media or the loss of membrane-bound hemoglobin in microvesicles [4, 29]. Much of the spontaneous hemolysis that occurs during storage consists of microvesicles [30]. Additionally, the presence of leukocytes in the red cell concentrates contribute significantly to an increase in hemolysis because of the release of various chemicals and enzymes, especially proteases from the leukocytes [31]. Not only the storage factors cause red cell hemolysis but also there are other factors that affect rate of hemolysis such as bacterial contamination, any disease of donor, mishandling of blood during processing, storage or shipping. Stored RBCs from blood donors with glucose-6-phosphate dehydrogenase deficiency, thalassemia, sickle cell ane-

mia, sickle cell trait or other forms of hemoglobinopathies possibly hemolyze more than average. Bloods from uremic and diabetic patients are more prone to mechanical damage, so hemolysis during storage [32]. Time delay between the collection and separation of blood, temperature changes due to refrigerator faults during storage, shipping blood units in direct contact with solid ice are common possible reasons of supernatant hemoglobin in RBC units [4, 19].

As a consequence of hemolysis, free hemoglobin, unbound free heme and iron (Fe^{+2} ,Fe^{+3}) accumulate in the extracellular media [33, 34, 35]. Accumulation rate of supernatant hemoglobin constantly and slowly rises until day 21 [36], generally accelerates during the 4^{th} through 6^{th} week [37]. End-of-storage hemolysis is widely spread but, typically, the range of hemolysis at day 42 is 0.2% to 0.6% in the presence of standard additive solutions [4, 15, 36, 38, 39, 40, 41]. In a review of data from 13,820 red cell units at the end of storage, hemolysis was found on the average of 0.35% [19].

In addition, decreasing of surface CD47 which inhibits macrophage activation and prevents phagocytosis of RBCs [42], moving of phosphatidylserine (PS) from the outer to the inner leaflet of membrane that leads to increase apoptosis, oxidative damage to glycoprotein Band 3 which have role in triggering immune removal mechanism [43] and increasing of supernatant annexin V proteins which is an indicator of cell injury are encountered alterations during storage [44]. In stored RBCs the levels of S-nitrosothiol-hemoglobin (SNO-Hb) which involves in generation of nitricoxide (NO) that induces vasodilation and allow RBC flow to match oxygen demand in the circulation are depressed by a factor of 4 at 3 hour after collection [45] and they are no longer detectable by day 3 of storage [46, 47].

2.2 Clinical Impacts of Transfusion

Transfusion is never considered as a fully safe treatment. Although, clearly many developments have been made in the storage of blood products, blood banking strategies, biochemical, morphological, immunological changes during storage are believed

to be associated with post-transfusional adverse outcomes on patients. Adverse consequences of RBC transfusion include hemolytic reactions, non-hemolytic transfusion reactions, transfusion-mediated immunomodulation, transmission of infectious agents and contaminated RBCs [48]. RBC transfusion is also associated with an increased risk of morbidity and mortality in critically ill, surgical and trauma populations [49].

Acute hemolytic reaction caused by accidental transfusion of ABO-incompatible RBCs remains a leading cause of fatal transfusion reactions [50]. The rate of mislabeled samples for the transfusion service has been measured 1000 to 10000 times more frequently than the risk of viral (HIV, HBV, HCV, HLTV) and bacterial infections from blood [51, 52]. Same rareness with transmission of infectios agents, allergic reactions and graft versus host diseases (GVHD) are encountered. GVHD occurs when T-lymphocytes in RBC transfusions engraft in an immunosuppressed recipient, usually occurs in transfusions between first degree relatives [51]. Those hazards of transfusion are not related to storage lesions of transfused blood.

Best way of categorizing complications of storage lesions is by dividing them into immune and non-immune mediated reactions. Immune mediated reactions include transfusion related immunomodulation (TRIM), febrile non-hemolytic transfusion reactions (FNHTR) and transfusion related acute lung injury (TRALI). The release of inflammatory or immunomodulating particles from leukocytes in stored blood, which leads to immunosuppressive effect on patient, is defined as TRIM. The responsible mechanism is thought to be related to apoptosis of blood cells over time with accumulation of bioactive substances that exert an anti-inflammatory effect within the recipient. The suspected bioactive substances are histamines, cytokines, lipids, microparticles and HLA-class I antigens. TRIM heightens the risk of infections and increased mortality [53]. FNHTR is not life threatening chill-fever reaction, but may cause discomfort to the patients. $Fn^{th}R$ may be due to the activation of donor leukocytes by HLA antibodies in the recipient [54]. TRALI is characterized by acute respiratory distress, noncardiogenic bilateral pulmonary edema and hypoxemia that occur within 1-2 hours after transfusion. TRALI may be due to the accumulation of neutrophils in the patient's pulmonary microvasculature and activation of those neutrophils with

accumulated stored blood component, CD40L, which cause endothelial damage, hence pulmonary oedema [55].

Hemolysis leads to both immune mediated and non-immune mediated events. Immune effects of RBC transfusions have largely been considered to be mediated by adaptive immune response. However, innate immune system; containing genetically preprogrammed cells and proteins that recognize and respond to harmful molecular species which are generally PAMPs (pathogen-associated molecular pattern) and DAMPs(danger associated molecular pattern molecules), is also responsible for transfusion related reactions. Heme and products of hemolysis can be transformed into DAMPs which activate the innate immune cellular response and may injure tissues and organs such as kidney and liver [33].

Accumulation of supernatant hemoglobin, hemoglobin encapsulated microparticles and unbound free heme as a consequence of hemolysis affect NO levels which has several major roles in physiologic signaling. NO is made in endothelial cells and controls blood flow by effecting smooth muscle relaxation adjacent to the blood vessels [56]. Free hemoglobin in hemolyzed RBC unit consumes NO by fast and irreversible reaction and reduces NO levels thus inhibits the vasodilatory response. Hb-encapsulated microparticles flow close to the endothelium, bring Hb close to the sites of NO synthesis and further NO scavenging occurs [57]. Although there are several mechanism such as reacting of Hb located inside the membrane of erythrocytes with NO to prevent the depletion of NO [47], free Hb and microparticles react about 1000 times faster than other mechanisms [58]. Thus, NO bioavailability decreases upon hemolysis and endothelial vasomotor function, blood cell adhesion and homeostasis are all adversely affected. Hypertension, increased systemic and pulmonary vascular resistance, even morbidity and mortality may occur [59].

Repeated transfusion of hemolyzed units may result in iron overload. With hemolysis, unbound iron accumulates in extracellular media. It can cause organ damage by formation of its deposits in the myocardial, liver and pancreatic tissues [35, 60].

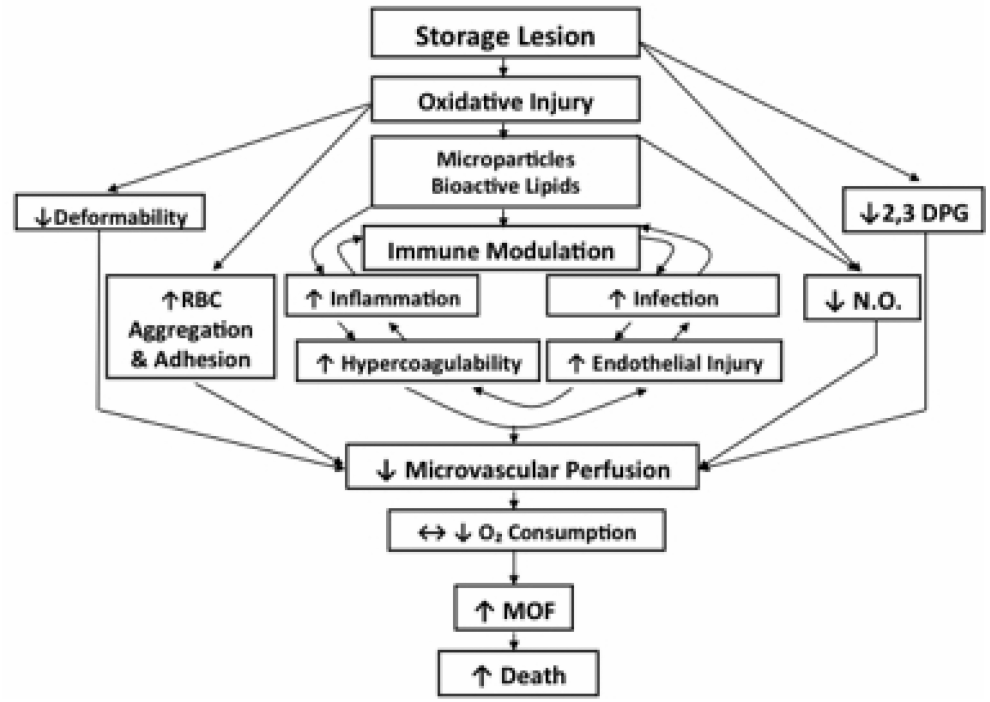

Figure 2.2 Schematic illustration of storage lesions and consequences [61].

As a non-immune mediated transfusion outcome, fast and large volume of transfusion cause transfusion related circulatory overload (TACO) which is characterized by congestive heart failure and acute pulmonary edema and results from incapacity of the heart to adequately pump the additional blood volume through the circulation [62].

One of the most important non-immune mediated adverse effects of transfusion is unimproved tissue oxygenation due mostly to 2,3-DPG depletion. Clinical and animal studies demonstrated that no significance change is observed in cardiac output or O_2 consumption, after transfusion of 2,3-DPG depleted blood [63]. Another study shows even a decrease in tissue oxygenation in critically injured trauma patients [60, 64].

Storage lesions influence flow properties of RBCs. As RBC deformability decreases during storage, RBC passage through the capillaries is affected. Erythrocyte suspensions with reduced deformability can impair perfusion, and thus oxygen delivery to peripheral tissues. Moreover, rigid RBCs can block capillaries. Increased RBC aggregability and RBC adhesion to endothelium also results in same consequences, in particular to patients with microcirculatory diseases [65]. Excess potassium in red cell

supernatant as a result of storage lesion is final non-immune mediated outcome of transfusion, cause hyperkalemia-related cardiac problems, especially in neonates [60, 66].

2.3 Solutions for Reducing Adverse Effects

Transfusion medicine has been exponentially improving since the first successfull transfusion attempt was made in 17^{th} century [67]. Researchers propose new solutions to improve storage, preparation, administration of bloods and experiments are performed to understand physiological events behind storage lesions. There are numerous techniques that minimize or eliminate the adverse effect of transfusion.

Many of the adverse effects associated with the transfusion of allogeneic RBCs have been shown to be related to the infusion of white blood cells (WBCs) present in stored blood [52]. Prestorage leukocyte filtration which is generally called leukoreduction is expected to reduce the release of most leukocyte derived cytokines, intracellular enzymes which have the potential to induce storage lesions in RBCs [68]. Via filters more than 99.995% of WBCs in the collected unit are removed and less than a million of WBCs are transfused [52]. Leukoreduction tends to reduce storage hemolysis by about 50% [41] and minimize the risks of FNHTR [69], TRIM and TRALI [55]

Different types of preservative and anticoagulant solutions have been developing in order to extend the expiration date beyond 6 weeks by upgrading the initial storage conditions. pH of the RBCs decreases through the storage period. Several physiological changes including reduction of ATP concentration follow this consequence. Reducing the amount of CPD anticoagulant is considered to maintain a higher initial pH [40]. An alkaline additive solution which is phosphate-adenine-glucose-guanosine-saline and mannitol (PAGGSM) was recommended recently so as to increase initial pH (8.2) [70]. Another experimental storage solution, EAS-81, contains adenine, dextrose, mannitol, sodium phosphate, and sodium bicarbonate. Preliminary studies indicate that less hemolysis, better morphology and more ATP concentration were obtained at the end of storage with EAS-81 [47]. PAGGSM and EAS-81 are not only decrease storage

lesions, but also extend expiration date to 7 and 8 week, respectively [40].

Rejuvenation is a poststorage treatment which aims to reverse storage-induced damage. According to the researches, rejuvenation improves ATP, 2,3-DPG levels, deformability so the circulatory functions in recipients [65]. Rejuvenation is also known as cell washing, has important added benefit of plasma removal and the associated prevention of most transfusion reactions caused by the accumulated substances in plasma [30]. A commercial rejuvenating solution (Rejuvesol) containing phosphate, inosine, pyruvate, and adenine, has been approved by FDA [65].

There are many other proposed blood management procedures to improve transfusion outcome. Gamma-irradiation is performed to minimize the risk of GVHD for immunocompromised patients and patients that relative of the donor [22]. Selected RBCs are gamma irradiated with minimum 25 Gy as a recommended dose so as to inactivate donor lymphocytes [71]. Pathogen reduction technology (PRT) is a relative new concept in blood banking, the aim of PRT is to inactivate any transfusion transmissible infectious agents, such as viruses and bacteria in RBC [13]. Yoshida *et al.* concluded that near complete removal of oxygen from RBCs during storage eliminated oxidative damage as a storage lesion and anaerobic conditions permitted 9 weeks of storage [72]. Cooling of whole blood rapidly after bleeding was suggested by Llohn *et al.* As a result of their study, fall in 2,3-DPG can be delayed significantly by cooling whole blood prior to storage [73]. Besides, an interesting recommendation was made about the usage of fresh blood instead of old bloods. After discovering the correlation between blood age and mortality, Purdy *et al.* indicated that for critically ill patients RBC stored for 14 days or less might be preferred [74].

2.4 Previous Studies About Quality Assessment of Blood Products

In contrast to the declared benefits of leukoreduction, rejuvenation, addition of preservative solutions and gamma-irradiation, many studies have claimed that their advantages are minimal [75] or those techniques have side effects on RBC viability [4, 76]. For instance, leukoreduction filters used prior to storage cause RBCs to lyse while passing through WBC filters. Rejuvenation process is expensive and time consuming [77]. PAGGSM has minimal advantage over SAGM [78]. Even though gamma irradiation is an essential technique for minimizing the risk of GVHD and very efficient to reduce immune-mediated reactions; it was proved that gamma irradiation increases RBC membrane permeability and speeds up K^+ leakage [79]. Cutting off storage at the end of second or third week of storage is not an adequate solution to reduce adverse transfusion outcomes since age of blood does not indicate quality of blood, even fresher bloods may cause transfusion related reactions [80]. Especially, in Istanbul, the need for blood donation is enormous and the number of blood transfusion minus the number of blood donation in a mon^{th} is negative.

Quality assessment of blood products prior to infusion is a propounded strategy in blood banking which also motivates this study. With a practical, economic, safe and also accurate measurement method, quality of the RBCs can be determined and hospital staff can decide whether the blood should be transfused or not. Researchers have attempted to develop a system that analyzes blood in various ways and determines blood quality. After relation between storage lesions and electrical impedance parameters of stored blood had been expressed [81, 82], Sezdi and Ulgen modelled ATP, pH, K^+, Na^+, Cl^- changes in stored blood with electrical impedance measurements of erythrocyte suspensions [83, 84]. Lim *et al.* presented a critical shear stress as a new measure of RBC aggregation to monitor and control the quality of blood storage [85].

Since degree of hemolysis of the blood has been widely considered as a good quality indicator, most of the attempts have been made to measure the concentration

of plasma hemoglobin inside blood bag. Hemoglobin is much more sensitive to optical measurements and clinically numbers of optical methods are used to measure degree of hemolysis [5, 86]. However, non-invasive studies for measuring supernatant hemoglobin are more interesting, because non-invasive techniques provide safe and rapid measurement. Most similar to the aim of this study, Meinke *et al.* introduced a novel optical device that non-invasively measures the amount of free hemoglobin in the stored blood by measuring transmitted two monochromatic light beams at 560 and 700 nm [87]. They also suggested sphere spectroscopy to measure optical properties of stored blood. Measurement of the degree of hemolysis from whole blood without centrifugation was performed by Bermakai *et al.*. They presented a spectroscopic method by using visible light spectrum to measure absorbance and transmittance of light which indicate the degree of hemolysis [10].

In similar manner, the aim of this study is to measure color in XYZ color space and the other derived color spaces to assess the degree of hemolysis from outside of the blood bag and without centrifugation. The motivation is based on the current technique used in blood banks in assessing the hemolysis with visual inspection. Visual assessment of hemolysis is subjective and not accurate [3], even with the use of a color comparator, since the perception of color varies due to several reasons such as the field of view, spectrum of the light source which lightens blood bag. This study analyzes the correlation between the mathematical representations of colors measured each day and the degree of hemolysis measured by the standard spectrophotometric method.

3. COLORIMETRY

Colorimetry is the branch of color science concerned with specifying numerically the color of physically defined visual stimulus in such a manner that: (a) when viewed by an observer with normal color vision, under the same specification look alike, (b) stimuli that look alike have the same specification, and (c) the numbers comprising the specification are continuous functions of the physical parameters defining the spectral radiant power distribution of the stimulus [88].

3.1 Color Vision

Before discussing the concept of colorimetry, it is necessary to know about color vision of normal human eye. As the cross-section of the human eye is seen in Figure 3.1, retina lines most of the interior of eye ball and is the light sensitive layer of eye. There are two types of receptors on the retina one of them is responsible for the color vision which is called cones. The others are called rods. These receptors are not uniformly distributed on retina. Color vision is limited to stimuli seen within about 40^o of the

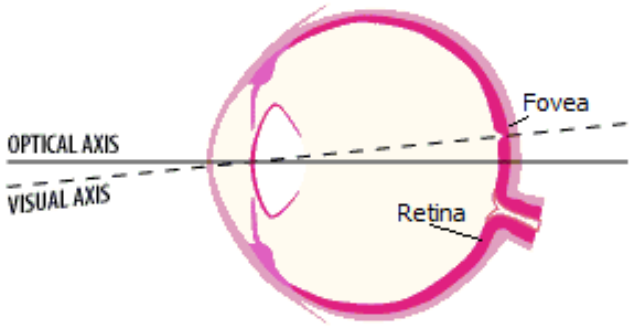

Figure 3.1 Illustration of visual and optical axis in human eye [89].

visual axis and within this angle the ability to see both color and fine detail gradually increases as the eye's axis is approached, the area of sharpest vision being termed fovea which comprises approximately the central 1.5^o diameter of the visual field. An area

within fovea, termed foveala and corresponds to a field of about 1^o. In the foveola, nearly all types of the receptors are cones.

There are three types of cones in retina. These are β, γ and ρ. Spectral sensitivities of these cones are shown in Figure 3.2. ρ cone has a maximum sensitivity in the yellow-orange part, the γ cone in the green part, and the β cone in the blue-violet part. These three types of cones are distributed more or less randomly in the retina. There are fewer β cones than ρ and γ; the ratios are estimated to be 40 to 20 to 1 for the ρ, γ and β cones, respectively. Color vision is basically three spectral weighting functions of these three cones, although the rods also provide a fourth spectrally different sense. Rods give monochromatic vision under low levels of illumination. Spectral sensitivity curve of the rods under low levels of illumination is plotted in Figure 3.2 as black line.

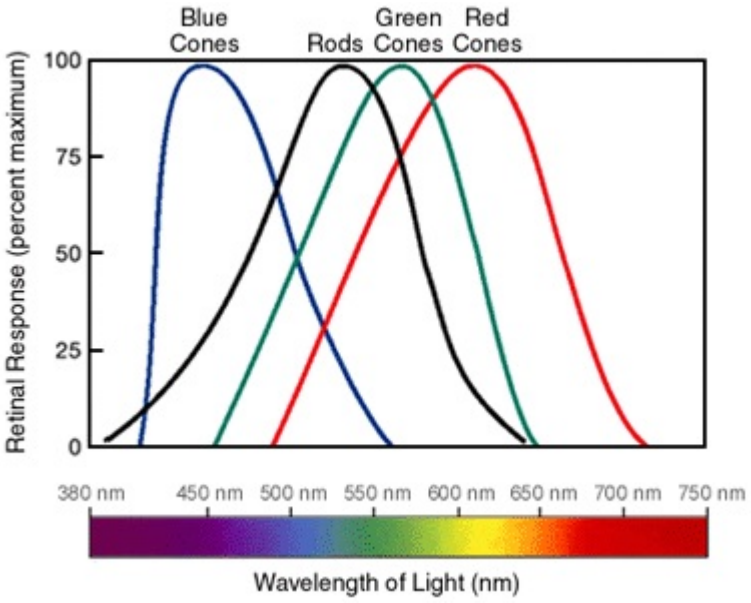

Figure 3.2 Spectral sensitivity functions of cones [90].

The human eye is to some extent capable of judging and comparing brightness or luminosity, an indicator of the amount of light striking the eye of the observer. The eye is not equally sensitive to all monochromatic radiations. Its sensitivity is higher for colors that are in the middle of the spectrum. Towards the extremities (red and

violet) the sensitivity gradually diminishes and becomes negligibly small in the infrared and ultraviolet regions. In order to attain the same brightness more radiant power of violet light has to be transmitted into the eye than yellow light. As a result, relative spectral luminous efficiency functions of the human eye for all wavelengths are formed as illustrated in Figure 3.3. Curve V'(λ) is spectral luminous efficiency function for low illumination condition; in the region of scotopic vision where only the rods are active. V(λ) corresponds to high illumination levels; that is in the region of photopic vision, where practically only cones are active.

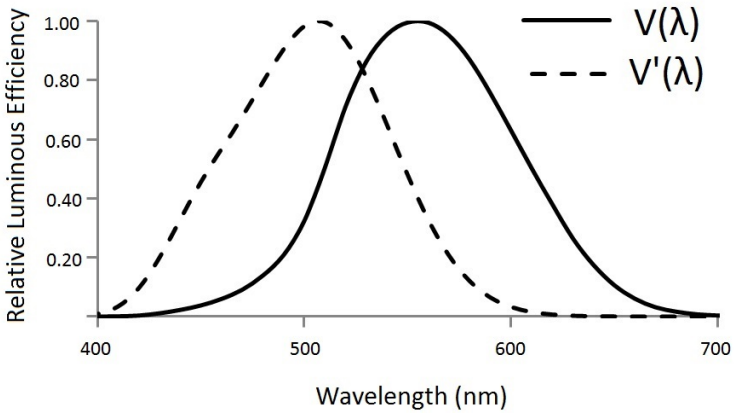

Figure 3.3 Relative spectral luminous efficiency function in the region of scotopic (V') and photopic vision (V) [91].

In order to include the sensation of brightness in the description of color, luminance has to be introduced. The definition of luminance for photopic vision is used in colorimetry because of the Purkinje phenomenon [92]. The luminance L is:

$$L = K_m \sum_n V_n P_n \tag{3.1}$$

where Km is a constant and equals 683 (lm W^{-1}), V_n is the spectral luminous efficiency and P_n is the power at n^{th} wavelength.

3.2 Historical Development of Color Spaces

The history of modern color science begins in 1666 when Isaac Newton began his research into this subject. Newton set up a color mixing apparatus that contains two prisms which separate white light into seven hues and two slits to select parts of the spectra in various ways and a movable screen for observing combined colors on it [93]. As a result of his experiment, Newton arranged all the colors of the spectrum around the periphery of a circle as shown in Figure 3.4. In his color plane, white is placed in the center on the diagram, while the points within the circle represented desaturated colors; the more desaturated the colors the closer they lay to the center. Newton also realized a third dimension was necessary which was intensity. 150 years after Newton, Grassmann expressed three fundamental laws in colorimetry.

Figure 3.4 Newton's color wheel [93].

Grassmann's first law was representation of colors in space [94]. Three matching stimuli; i.e. three relative spectral energy distributions, are so selected that it is impossible to match one of them by mixture of the other two. Any color stimulus; i.e. any relative spectral energy distribution of given luminance can be matched by additive mixing of the matching stimuli with suitable luminance. In the general formulation, matching stimuli are not necessarily monochromatic radiations as Maxwell used R (700

nm), G (546.1 nm), B (435.8 nm), they can be indicated as (1), (2), (3) in a general form (Figure 3.5). A color stimulus (K) can be characterized by the numbers L_1, L_2, L_3 being the luminance of three matching stimuli (1), (2) and (3).

$$(K) \leftrightarrow L_1(1) + L_2(2) + L_3(3) \tag{3.2}$$

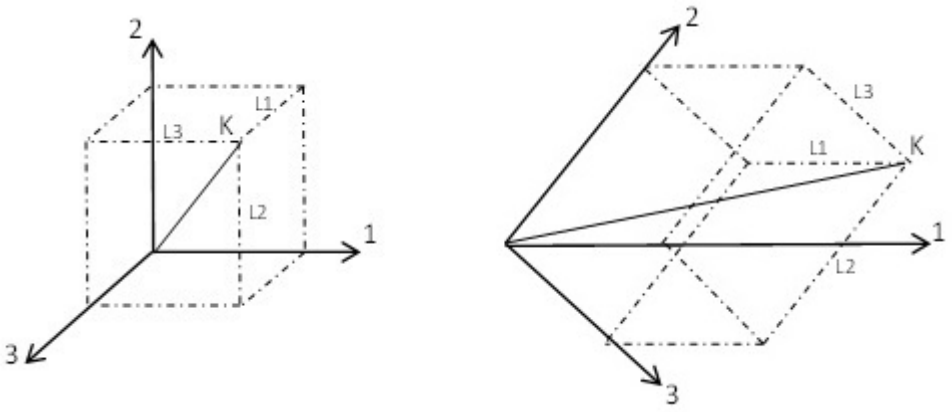

Figure 3.5 Grassmann's first law: Any color stimulus (K) can be represented in 3-dimensional coordinate system a) with matching stimuli (1), (2), (3) having right angles between each other and b) with oblique axes having smaller than 90^o.

These three axes can be chosen at right angles as in Figure 3.5a or with the axes forming three equal angles, smaller than 90^o, as in Figure 3.5b. In principle it has no consequence which of these two systems is chosen for the representation of color stimuli.

The second law of Grassmann reads: if two color stimuli match, they continue to do so if we increase or decrease the luminance of both by the same factor [94]. That means the equation 3.2 holds when all the luminance are multiplied by the same factor n:

$$n(K) \leftrightarrow nL_1(1) + nL_2(2) + nL_3(3) \tag{3.3}$$

With any change in the luminance of (K), the amounts of the matching stimuli required for the match change proportionally.

The third law of Grassmann says: "Two color stimuli, matching when displayed next to each other, act in exactly the same manner when mixed with other stimuli" [94]. This law is expressed in color equations as:

$$(K) \leftrightarrow L_1(1) + L_2(2) + L_3(3) \tag{3.4}$$

$$(K') \leftrightarrow L'_1(1) + L'_2(2) + L'_3(3) \tag{3.5}$$

$$(K) + (K') \leftrightarrow (L_1 + L'_1)(1) + (L_2 + L'_2)(2) + (L_3 + L'_3)(3) \tag{3.6}$$

Same years, James Clark Maxwell was the first to determine the color matching functions or tristimulus values for the visible spectrum experimentally [95]. Then he developed color triangle (Figure 3.6) and chromaticity diagram. According to his experiments and Newton's work, Maxwell added spectrum locus containing the color points for monochromatic stimuli on chromaticity diagram. In the Figure 3.6, the

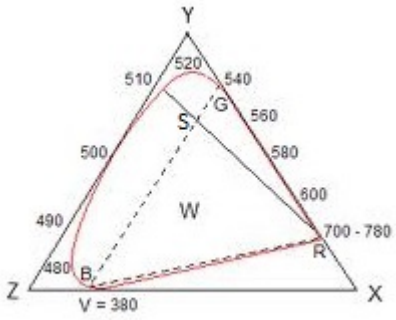

Figure 3.6 Color triangle [96].

numbers give the wavelengths. The triangle RGB indicates the monochromatic radiations 700 nm (red), 546.1 nm (green), 435.8 nm (blue) respectively. W is the point representing white. White point is equally distant to R, G and B. General mixing rule is that the mixtures of two colors are pointed on the line connecting these two colors. For example, the line BG, contains all colors that can be matched by mixtures of (B) and (G), the position of the point representing the mixture color is determined

by the percentages of the compositions. The distance between that point and one of the compositions of the color mixture is inversely proportional to contribution of that component. As seen in the Figure 3.6, many colors, particularly the monochromatic stimuli, are outside RGB triangle and they can not be produced by mixing red, green and blue in any proportion. However, the stimulus of wavelength 510 nm for instance can still be related to R, G and B. By mixing an amount "a" of the color of 510 nm with a suitable amount "r" of matching stimulus (R), color (S) with the amount "s" can be obtained:

$$a(510) + r(R) \leftrightarrow s(S) \tag{3.7}$$

This amount "s" of color (S) can also be reproduced by mixing an amount "g" of color (G) with an amount "b" of color (B):

$$g(G) + b(B) \leftrightarrow s(S) \tag{3.8}$$

It follows from the two color equations that:

$$a(510) + r(R) \leftrightarrow g(G) + b(B) \tag{3.9}$$

Hence we can reproduce a(510) by a negative amount of (R) plus two positive amounts of (G) and (B):

$$a(510) \leftrightarrow -r(R) + g(G) + b(B) \tag{3.10}$$

Monochromatic color stimulus of wavelength 510 nm is reproduced by a suitable mixture of (R), (G), (B). RGB color triangle system has disadvantages that some colors outside of RGB triangle in Figure 3.6 can not be reproduced without at least one negative coordinate. The primary points of the color triangle should be selected so that all colors and spectrum locus are comprised by the color triangle. Another drawback is the position of white point. The angles of the RGB tristimulus values should be arranged suitable for centering white point.

Colors in a chromaticity diagrams can also be represented in another way with their dominant wavelengths and colorimetric purity. Many of colors except the RWV triangle on the diagram (Figure 3.6), can be reproduced by mixing white and single monochromatic radiation on the spectrum locus. This wavelength to be used together with white for the reproduction is called dominant wavelength. Colorimetric purity is the luminance of monochromatic component of mixture with white to reproduce a color divided by the luminance of the reproduced color. Therefore, colorimetric purity of the color converges "1" when it approaches to spectrum locus and colorimetric purity of white is "0".

Improvement of trichromatic systems for defining colors was continued in 20^{th} century with Munsell and Ostwald's work. In 1915, Albert Munsell developed a three-dimensional color notation system in which he classified colors according to three perceivable qualities: hue, value and chroma [97]. Hue is that quality by which one color can be distinguished from another, as a red from a yellow, a green, a blue. Value is the lightness or darkness of the color. "0" is assigned for perfect black and "1" for white. The third term chroma is the intensity of the color. The chroma begins with a zero for neutral color and moves to high-numbered values as the color becomes more saturated. Hue, value and chroma in Munsell system respectively correspond to dominant wavelength, brightness and purity in chromaticity diagram.

Ostwald color system is very similar to Munsell system [98]. They both are called material system that involves the use of standard colored samples against which other colored materials can be compared. This type of measuring color is called visual inspection. However it has many disadvantages against another approach that is widely used to measure color, because of the phenomenon known as metamerism [99]. Other kind of system analyzes spectrum of light reflected from a surface and assigns a set of tristimulus values that specify the color with unique coordinates in a color space [100]. Thus the specification of the tristimulus values uniquely describes the color appearnce of a surface. With this system, any two surfaces that reflect spectra having the same tristimulus values will also appear the same color. CIE systems are examples of the systems analyzing the reflected light for specifying color.

3.3 CIE 1931 XYZ Color Space

In 1931, CIE (Commision Internationale de l'Eclairage) introduced XYZ color system by selecting Guild and Wright's experimental data [101, 102] as the basis of the system. Based on their results color matching properties of an ideal observer was defined by specifying three independent functions of wavelength, $\overline{x}(\lambda)$, $\overline{y}(\lambda)$, $\overline{z}(\lambda)$ and was called CIE 1931 Standard Colorimetric Observer (Figure 3.7). These color matching functions are used for calculating the tristimulus values X, Y and Z. From definition: If two color stimuli have the same tristimulus values X, Y, Z, they will look alike, when viewed under same phototopic conditions, by an observer whose color vision is not significantly different from that of the CIE 1931 Standard Colorimetric Observer; conversely, if the tristimulus values are different, the colors may be expected to look different in these circumstances. CIE 1931 Standard Colorimetric Observer is usually referred as 2^o observer. 2^o observer means the vision of the sample occurs inside foveala where the number of cones is maximum. There are also a specified color matching functions for 10^o observer which is developed in 1964, but they are used in large field of view. Color matching functions for 2^o observer are generally used one.

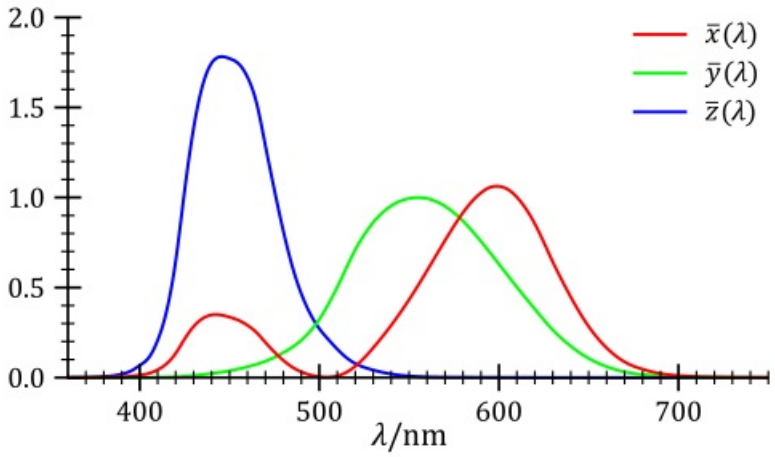

Figure 3.7 Color matching functions of 2^0 observer; $\overline{x}(\lambda)$, $\overline{y}(\lambda)$, $\overline{z}(\lambda)$ [103].

The color matching functions roughly define the spectral response functions of ρ, γ and β cones of standard colorimetric observer and the tristimulus values X, Y,

Z correspond to R, G, B in previous section. CIE XYZ system eliminates all the disadvantages in the RGB trichromatic system such as having negative intensities. The CIE XYZ system is derived from Grassmann's laws and very similar to RGB trichromatic system. As Grassmann's first law indicates in Figure (3.5b), three coordinate axes are formed the color space, but this time named X Y Z tristimulus values (Figure 3.8). They are comprises all the colors and spectrum locus. Luminance of the col-

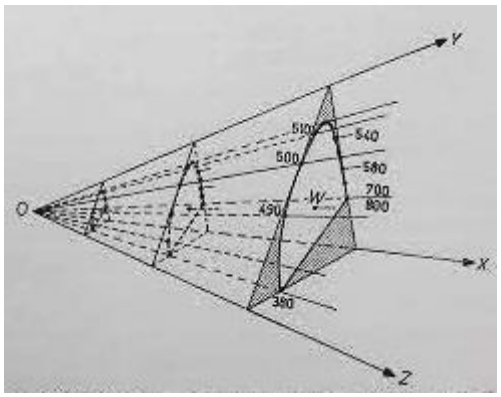

Figure 3.8 Spatial illustration of chromaticity diagrams on XYZ system [96].

ored object determines how far the chromaticity diagram (Figure 3.8) away from the origin (Grassmann's second law). Tristimulus values are calculated from their luminance components which is found from their corresponding matching functions so the equation of the tristimulus values are:

$$X = K_m \sum_n \overline{x}_n P_n \tag{3.11}$$

$$Y = K_m \sum_n \overline{y}_n P_n \tag{3.12}$$

$$Z = K_m \sum_n \overline{z}_n P_n \tag{3.13}$$

P_n is the spectral distribution of radiant power coming from the surface of the colored object. $\overline{x}(\lambda)$, $\overline{y}(\lambda)$, $\overline{z}(\lambda)$ are the color matching functions of XYZ system.

CIE XYZ color space reveals another advantage of it that one of the color matching functions $\overline{y}$ coincides with standard $V(\lambda)$ function which is the sensitivity

function of the rods in photopic vision (Figure 3.2). The $\overline{y}$ function has the same shape as, but also identical to, V(λ) function. As a consequence, according to the equation 3.1 the tristimulus value Y is the luminance of the color stimulus. Brightness sensitivity of human eye is constructed into the XYZ system with matching function $\overline{y}$.

The tristimulus values X, Y and Z specify the color of a given spectrum. On the other hand, it is difficult to understand the color of sample when its tristimulus values are presented. The reason of this is about Grassmann's second law; tristimulus values determine only the coordinates of the chromaticity plane in XYZ space. The coordinates of the color are calculated in the chromaticity diagram from the relative magnitudes of the tristimulus values.

$$x = \frac{X}{X+Y+Z} \tag{3.14}$$

$$y = \frac{Y}{X+Y+Z} \tag{3.15}$$

$$z = \frac{Z}{X+Y+Z} \tag{3.16}$$

Lower case letters are always used for the chromaticity coordinates and they represent the relative amounts of the tristimulus values. From the above expressions it is apparent that;

$$x + y + z = 1 \tag{3.17}$$

This means the chromaticity coordinates (x, y, z) only contain two independent numbers, third is dependent to other two. The chromaticity diagram is constructed with only two variables x and y, as two dimensional plane (Figure 3.9). This diagram provides a sort of color map on which the chromaticities of all colors can be plotted. Alternative to XYZ system, description of a unique color stimulus can be made with its chromaticity coordinates x and y and its brightness value Y. Also, dominant wavelength and colorimetric purity instead of x and y coordinates gives a unique color

description in the chromaticity diagram. The point S_E in the chromaticity diagram represents the equi-energy stimulus so that its chromaticty coordinates are x=$\frac{1}{3}$, y=$\frac{1}{3}$ so z.

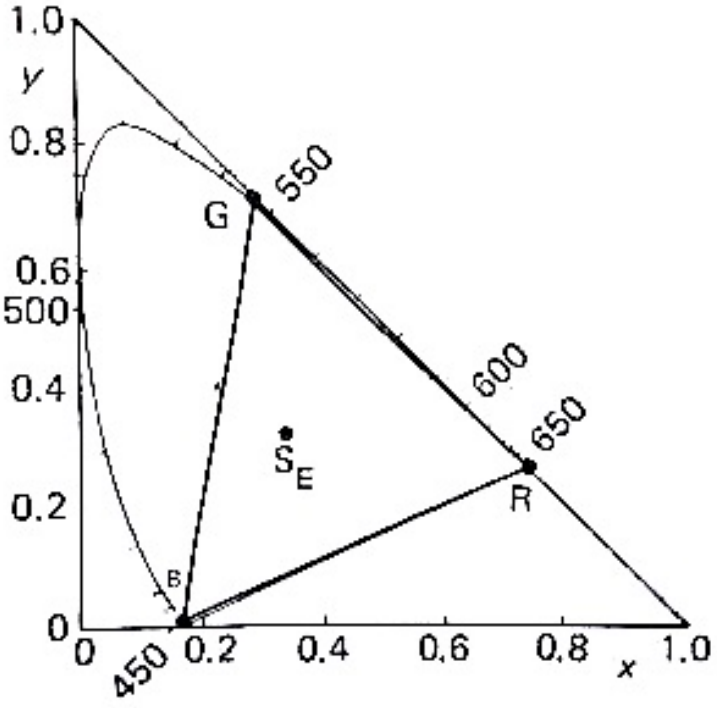

Figure 3.9 The point S_E in xy chromaticity diagram [104].

3.4 Light Sources

Light sources play a very important part in colorimetry. Light emitted from a source of a radiant power, such as the sun or incandescent lamp, strikes a given sample and makes the sample visible to the observer. The color stimulus emerging from the sample and entering observer's eye produces a sensation of color which the observer identifies as the color of the sample. Thus, the spectrum of the light coming from a given sample depends on the spectrum of light that illuminates the sample. The nature of light sources profoundly affects the appearance of colored sample. For example, under illumination with sodium lamp objects that are normally red, appears dark brown or black. Different types of illumination produce different set of chromaticity coordinates

and tristimulus values as expressed in equations (3.11),(3.12),(3.13). Color points of light sources lie in a wide region about the point S_E (x=$\frac{1}{3}$, y=$\frac{1}{3}$) in chromaticity diagram (Figure 3.9).

3.4.1 Standard Illuminants

CIE have decided to define a set of spectral radiant power distributions called CIE standard illuminants, in order to reproduce spectral energy distribution accurately for a given illuminant in any laboratory and specify the exact color points of illuminants in the color spaces. There are dozens of standard illuminants which are A, B, C, D_{55}, D_{65}, D_{75}, E and illuminants for fluorescent lighting F_1 to F_{12}.

Standard illuminant A represents the light from tungsten lamp. Tungsten lamp is a convenient standard because the spectral power distribution of its light is entirely dependent on the temperature of its filament. Standard illuminant A is defined as light from the Planckian radiator at absolute color temperature 2856 K. Color temperature is the temperature of a Planckian radiator whose radiation has the same chromaticity as that of a given stimulus.

Standard illuminant B represents sunlight with a correlated color temperature (CCT) of about 4874 K and standard illuminant C represents average daylight with CCT of approximately 6774 K. CCT is the temperature of the Planckian radiator whose perceived color most closely resembles that of a given stimulus seen at the same brightness and under specified viewing conditions. Nevertheless, both illuminant B and C were considered inadequate in representing the intended phases of natural daylight and dropped from the list of recommended standard illuminants published by CIE in 1971 [105]. Instead, CIE standard illuminant D_{65} is widely used as the representative of daylight for colorimetry. Standard illuminant D_{65} has CCT of about 6504 K and as a series of D illuminants; D_{50}, D_{55} are designated for daylights having CCT of about 5000 K, 5500 K, respectively.

3.4.2 Standard Sources

CIE distinguishes between sources and illuminants. Whereas a source refers to a physical emitter of radiant power such as a lamp or the sun, an illuminant refers to a specific spectral radiant power distribution incident on the object viewed by the observer. The spectral radiant power distribution of an illuminant may not necessarily be exactly realizable by a source. Sources are needed to conduct visual colorimetry or color measurements by means of physical colorimeters.

CIE standard source A that realizes standard illuminant A is as mentioned tungsten filament lamp operating at a color temperature 2856 K. However, there are no artificial sources that realize the D illuminants due to their unique and jagged spectral distribution. By using color difference formula, CIE assessed the usefulness of existing artificial sources as a simulator for D illuminants. One of the daylight simulators which is recommended by CIE is tungsten-halogen lamp which is used in this study.

3.4.3 Tungsten-halogen Lamp

Ordinary tungsten lamp evaporates from the filament, forms a dark deposit on the glass envelope and weakening it. A tungsten-halogen lamp attains a much higher temperature when the lamp is running. The envelope contains a halogen gas and the evaporating tungsten combines with it. Then, this combined gas migrates back to the filament decomposes to deposit the tungsten back on to the filament and halide back into the envelope. Thus the halide provides a continuous cycle of protection from dark deposits on the envelope and prevents reduction of the filament. This means that the filament can be run at a higher color temperature at about 3300 K. Spectral radiant power distributions of tungsten-halogen lamp correlates well with illuminant D_{65}.

3.4.4 White Diffuse Reflectance Standard

CIE recommends perfect reflecting diffusers that reflect all visible monochromatic radiations well and equally. For instance magnesium oxide surface which is used in this study reflects up to 98 percent of the incident light.

3.5 Other Color Spaces

Several attempts were made to describe colors mathematically in a color space in various ways since CIE XYZ system has some disadvantages. One of them is non-uniformity in distribution of colors in chromaticity diagram. In order to represent color differences with equal distances in chromaticty diagram and improve XYZ system, several color spaces have been proposed.

3.5.1 Hunter Lab Space

The Hunter Lab color space was developed in 1948 by Richard S. Hunter as a uniform color space which could be read directly from a tristimulus values (Hunter L, a and b). Main property of Hunter Lab is uniformity. Uniform color space is a color space in which equal distances on the coordinate diagram correspond to equal perceived color differences. In Hunter Lab, there are three axes in three dimensional Cartesian coordinate system which are labeled L, a, and b as seen in Figure 3.10. The Hunter Lab color space incorporates the opponent-colors theory (see E. Hering, 1878) with a-axis representing the redness or greenness of a color and the b-axis representing the yellowness or blueness of a color. The L-axis represents the perceived lightness of the color. Coordinates of Hunter Lab space are calculated from the measurement of the CIE 1931 XYZ tristimulus values:

$$Hunter\, L = 100\sqrt{\frac{Y}{Y_0}} \tag{3.18}$$

$$Hunter\, a = 175\sqrt{\frac{0.0102}{Y/Y_0}}\left[\left(\frac{X}{X_0} - \frac{Y}{Y_0}\right)\right] \tag{3.19}$$

$$Hunter\, b = 70\sqrt{\frac{0.00847}{Y/Y_0}}\left[\left(\frac{Y}{Y_0} - \frac{Z}{Z_0}\right)\right] \tag{3.20}$$

where the tristimulus values X_0, Y_0, Z_0 are those of the nominally white object color stimulus. Usually, the white object color stimulus is given by the spectral radiant power of one of the CIE standard illuminants, in this study, D_{65}, reflected into the observer's eye by the perfect reflecting diffuser. Under these conditions, X_0, Y_0, Z_0 are the tristimulus values of the standard illuminant with Y_0 equal to 100.

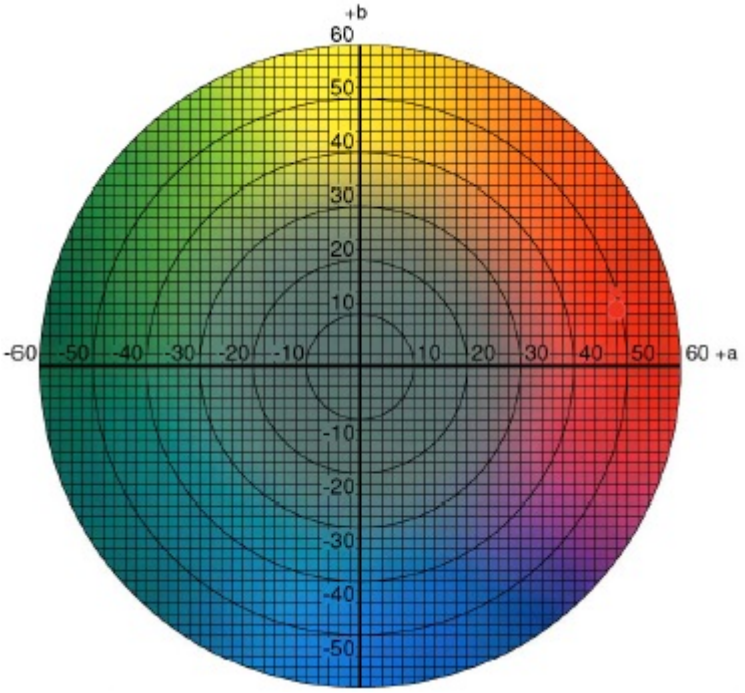

Figure 3.10 Hunter Lab Space [106].

3.5.2 CIE 1960 Yuv Space

Yuv is a linear transformation of XYZ system, in an attempt to produce a chromaticity diagrams in which a vector of unit magnitude is equally visible at all colors. Non-uniformity of XYZ chromaticity diagram is reduced considerably, but not

enough. Transformation equations of the chromaticity coordinates u, v are expressed as in the following:

$$u = \frac{4X}{X + 15Y + 3Z} \tag{3.21}$$

$$v = \frac{6Y}{X + 15Y + 3Z} \tag{3.22}$$

Y is unchanged from XYZ system, but is not defined as luminance, it represents lightness index. Today, the CIE 1960 UCS is mostly used to calculate CCT, where the isothermal lines are perpendicular to the Planckian locus.

3.5.3 CIE 1964 U'V'W' Space

The CIE 1964 (U', V', W') color space, also known as CIEUVW, is an extension of the CIE 1960 Yuv system in an attempt to obtain a color solid for which unit shifts in luminance and chrominance are uniformly perceptible. The variables, U' V' W', plotted along mutually perpendicular axes to produce uniform color space, are nonlinear transformations of the chromaticity coordinates x, y and luminous reflectance Y. u' and v' represent the axes of the chromaticity diagram which is similar to chromaticity diagram of XYZ system (Figure 3.11).

$$W' = 25\sqrt[3]{Y} - 17 \tag{3.23}$$

$$U' = 13W'(u - u_0) \tag{3.24}$$

$$V' = 13W'(v - v_0) \tag{3.25}$$

where u_0 and v_0 are the chromaticity coordinates of the reference illuminant. W' is defined as a lightness index.

$$u' = CIE\,1960\,u = \frac{4X}{X + 15Y + 3Z} \tag{3.26}$$

$$v' = 1.5(CIE\,1960\,v) = \frac{9Y}{X + 15Y + 3Z} \tag{3.27}$$

Since chromaticity diagram of XYZ system is non-uniform, colorimetric purity and

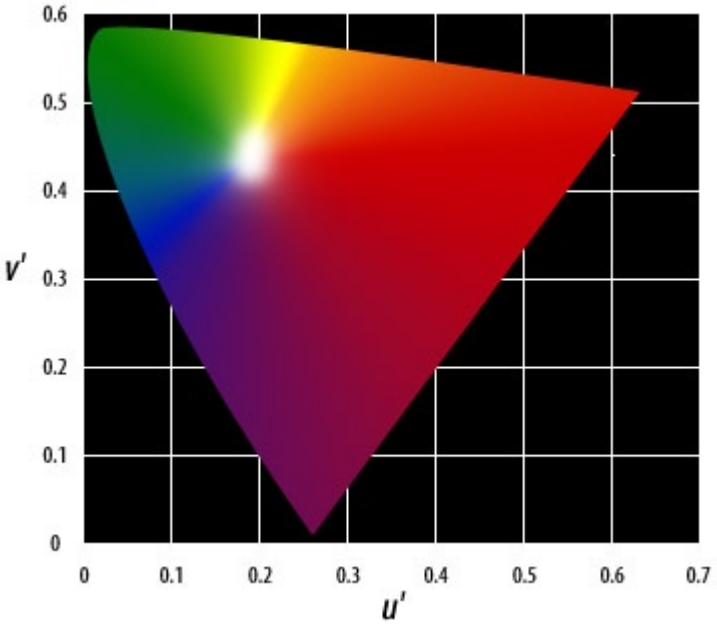

Figure 3.11 u'-v' chromaticity diagram [107].

dominant wavelength do not correlate uniformly with the perception of saturation and hue respectively. Two new measures have been provided, based on u' v' diagram that correlate with hue and saturation more uniformly. They are u-v hue-angle and u-v saturation:

$$u, v\,hue\,angle = \arctan\left[\frac{v' - v_0}{u' - u'_0}\right] \tag{3.28}$$

$$u, v\,saturation = 13\left[\left(u' - u'_0\right)^2 + \left(v' - v'_0\right)^2\right)\right] \tag{3.29}$$

where u'$_0$ and v'$_0$ are the values of reference illuminant in u'-v' diagram.

3.5.4 CIE 1976 L*a*b* Space

One of the uniform color spaces, CIELAB is an opponent color system based on the earlier Hunter Lab. Color opposition correlates with discoveries in the mid-

1960s that somewhere between the optical nerve and the brain, retinal color stimuli are translated into distinctions between light and dark, red and green, and blue and yellow. The color axes of CIELAB are constructed according to this theory. In three dimensional L* a* b* space (Figure 3.12), L* represents lightness whose values run from 0 (black) to 100 (white). On the a* axis, positive values indicate amounts of red while negative values indicate amounts of green. On the b* axis, yellow is positive and blue is negative. For both axes, zero is neutral gray.

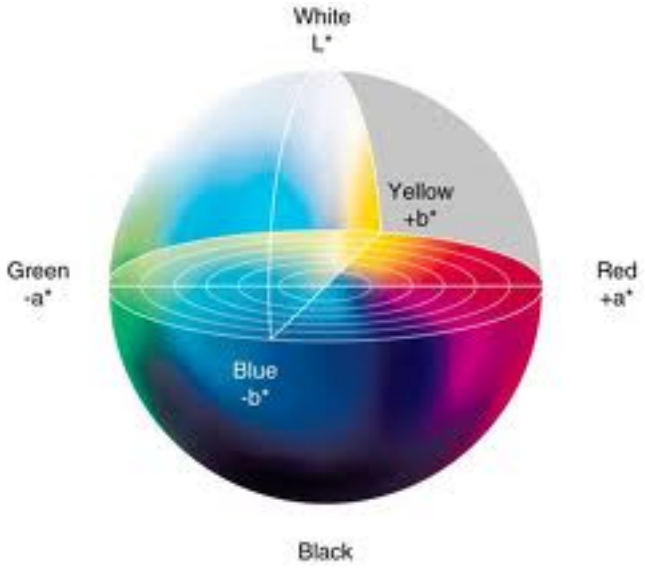

Figure 3.12 CIE Lab Space [108].

The difference between Hunter and CIE color coordinates is that the CIE coordinates are based on a cube root transformation of the color data, while the Hunter coordinates are based on a square root transformation. The color axes of CIE L*a*b* space are defined as:

$$L* = 116f\left(\frac{Y}{Y_0}\right) - 16 \tag{3.30}$$

$$a* = 500\left[f\left(\frac{X}{X_0}\right) - f\left(\frac{Y}{Y_0}\right)\right] \tag{3.31}$$

$$b* = 200\left[f\left(\frac{Y}{Y_0}\right) - f\left(\frac{Z}{Z_0}\right)\right] \tag{3.32}$$

where,

$$f(s) = \begin{cases} \sqrt[3]{s} & \text{for } s > 0.008856 \\ 7.787s + 0.1379 & \text{for } s \leq 0.008856 \end{cases} \tag{3.33}$$

In these formula, the reduced perceptual significance of a given difference in chromaticity caused by a reduction in luminance factor is incorporated by using the tristimulus ratios X/X_0, Y/Y_0, Z/Z_0 instead of chromaticity coordinates. Since these ratios of the tristimulus values are incorporated as cube roots, there is no chromaticity diagram associated with the CIELAB space. Therefore CIELAB space lacks direct correlation with older concepts of saturation. However, correlates of hue and chroma are available and formulated as:

$$CIELAB\,hue\,angle = \arctan\left(\frac{b*}{a*}\right) \tag{3.34}$$

$$CIELABchroma = \sqrt{a*^2 + b*^2} \tag{3.35}$$

4. MATERIALS AND METHODS

4.1 Volunteers

Ethical approval was obtained from Human Research Ethical Committe, Bogaziçi University for studying the blood products of the participants. 7 adult male donors aged 29±6.68 years gave their consent to participate in this study. Only male donors were selected because blood products of male donors hemolyze more than female ones [32]. Donors were taken to the transfusion center at Florence Nightıngale Hospital, Şişli, İstanbul. Two samples were collected from each donor; for complete blood count and infection disease tests. As in every blood donation process, clinician physically examined the donor and checked complete blood count before drawing blood.

4.2 Red Blood Cell Preparation and Storage

Approximately, 450 ml of blood were drawn into a blood bag containing 63 ml of anticoagulant solution, CPDA. Following collection, whole blood rested for 10 minutes and then centrifuged for separating plasma from cells. After 15 minutes of centrifugation, plasma and some buffy-coat were manually extracted into another bag connected to the main bag, in which whole blood was collected. The connection was then cut with a sealer and the plasma disposed. 100 ml of preservative solution (SAGM) was added on RBCs and RBC suspension was obtained. Leukoreduction was not applied on any blood product. RBC concentrates were transported with a blood transporter bag containing liquid cooler. RBC concentrates were not connected directly to cold surface so as not to damage red blood cell membrane and cause hemolysis. RBCs were stored at 4±0.5 ^{o}C, in a blood bank refrigrator (Panasonic MBR-107) with a continuous temperature recording system and vibrationless motor; to avoid additional hemolysis. Each day, color measurements were performed non-invasively and; each week, 5 ml of blood samples were drawn to measure the degree of hemolysis by the golden standard

i.e. Harboe technique.

4.3 Instruments

Instruments for color measurements; are namely, special light source, fiber optic reflectance probe, probe holder, white diffuse reflectance standard and a spectrophotometer (Figure 4.2). Tungsten-halogen light source (HL-2000 OceanOptics) which has a very close spectral power distribution to standard illuminant D_{65}, has a wavelength range of 360 nm to 2400 nm. Color temperature of the light source is 2960 K. Fiber optic reflectance probe(R200-7 OceanOptics) consists of a tight bundle of 7 optical fibers, 6 illumination fibers around 1 read fiber (Figure 4.1). The diameter of each

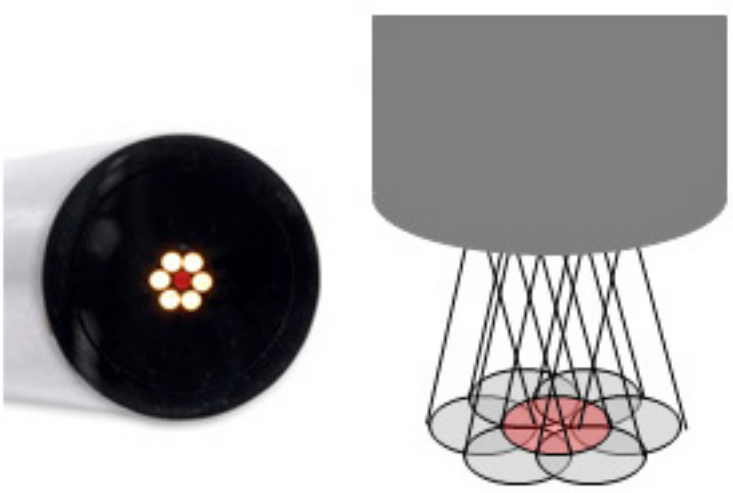

Figure 4.1 View of reflection probe and optical paths of 7 optical fibers [109].

fiber is 200 μm. The probe has two legs at opposite ends and are connected to the light source and the spectrometer. The reflection probe holder (RPH-1 OceanOptics) is an anodized aluminum platform, with a machined hole at 45^o. White diffuse reflectance standard (WS-1 OceanOptics) is made up of polytetraflouroethylene (PTFE) that reflects >98% of incident light, from 250 nm to 1500 nm. The spectrophotometer (USB4000 OceanOptics) used in the experiments can measure both visible and near infrared light intensity up to 65000 photons over a predetermined integration time.

The spectrophotometer has a detector range of 340 nm to 1030 nm. Data transfer and recording are made possible with USB connection to the computer and by using the software SpectraSuite (OceanOptics) that is compatible with Windows and Linux operating systems. SpectraSuite has also a color measurement module, for computing all color space coordinates and related parameters from relative reflection spectrum.

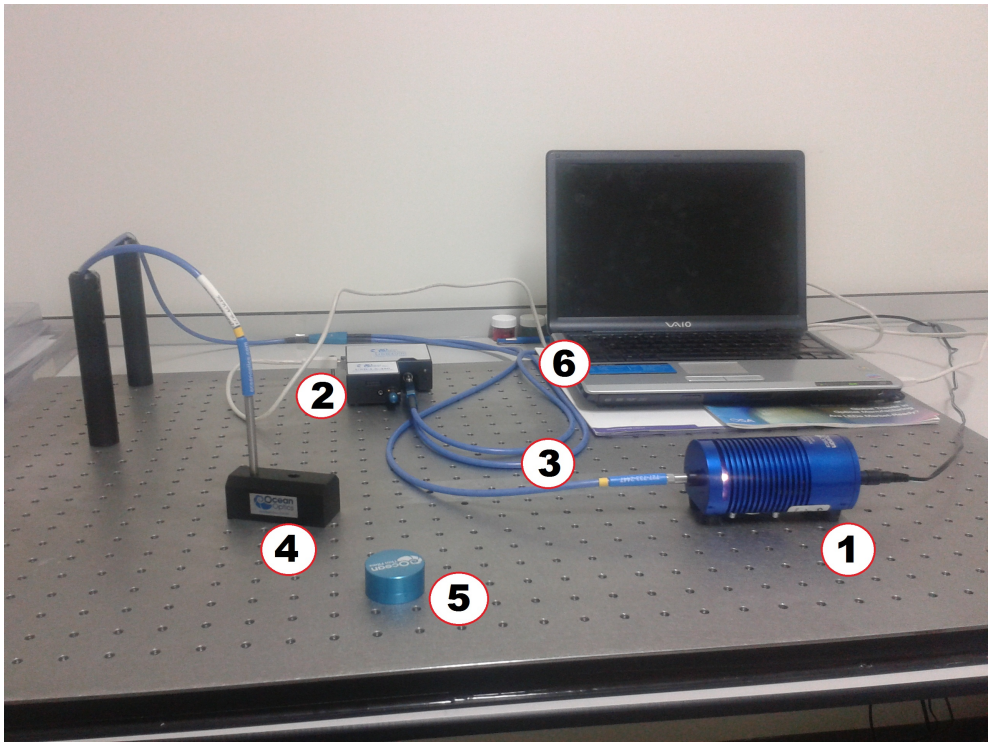

Figure 4.2 The instruments used in color measurement: light source(1), spectrophotometer(2), reflection probe(3), reflection probe holder(4), diffuse reflectance standard(5), and computer(6) in which the software installed.

Measurements of hemolysis with Harboe technique were performed in a clean room environment to avoid any bacterial contamination. Besides fundamental laboratory equipments, microplate spectrophotometer (μQuant Biotek) was used for spectrometric method for measuring the extracellular plasma content. The microplate spectrophotometer can read the absorbance of liquid samples at single wavelength with a monochromator of very high accuracy ($\pm$2 nm) and repeatibility ($\pm$0.2 nm). The wavelength range of this spectrophotometer is from 200 nm to 999 nm.

4.4 Color Measurement

Beginning from 0^{th} day of storage, tristimulus values and color coordinates in various spaces: CIE XYZ, Yuv, U'V'W', L*a*b* and Hunter Lab; and other colorimetric parameters such as CIELAB chroma, color temperature were recorded and their changes throughout the storage period were observed.

On each day of storage, totally 24 colorimetric parameters, most of which are dependent of the independent tristimulus values (X, Y, Z), were measured. Color of stored blood was measured from the transparent surface of the blood bag. In color measurement, the reflection probe holder was positioned at the mid level of the blood bag and the reflection probe was placed at 45^o aperture of the probe holder (Figure 4.3). Other ends of the probe were connected to the spectrophotometer and the

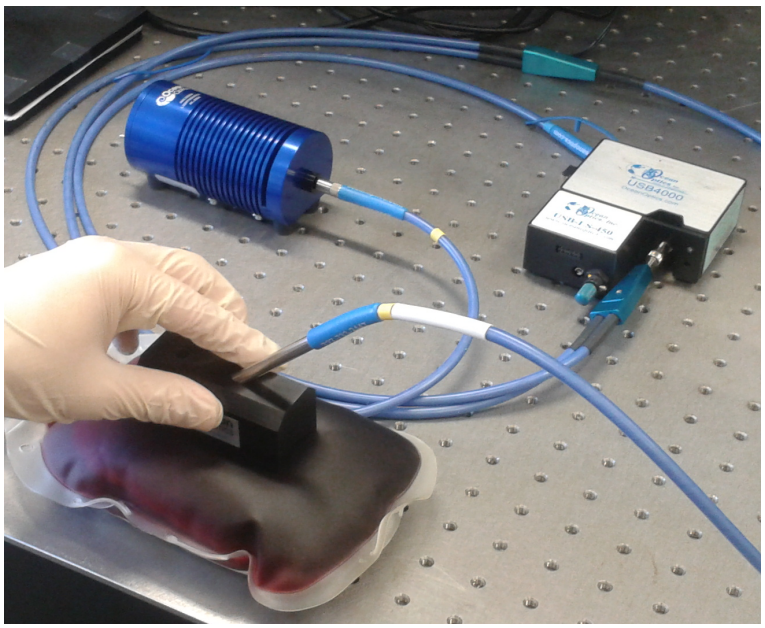

Figure 4.3 Color measurement.

light source. By this way, the incident light from the light source was transmitted through the blood bag; and reflected light from the blood bag measured with the spectrophotometer. Finally, the software calculated all colorimetric parameters according to relative reflectance.

Before measurements, the light source was switched on for minimum 20 minutes for warm up and settlement. Experimental mechanism was set up in a dark room. In the software, an appropriate integration time, boxcar width and scans to average values were selected. Boxcar width was selected 5, as it corresponds to 1 nm. Number of scans to be averaged was selected not more than 20 scans in order not to increase measurement time. Dark spectrum and reference spectrum were recorded by the software before measuring RBC concentrates. Reference spectrum was measured by placing diffuse reflectance standard under the probe holder (Figure 4.4). Finally 2^o observer

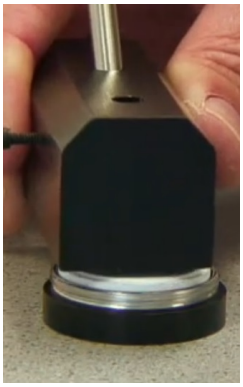

Figure 4.4 Measurement of reference spectrum.

was selected due to the small field of view and D_{65} was selected for the illuminant. Color measurement of RBCs was ready, but before beginning, the reference spectrum was checked by the diffuse reflectance standard. The experiment started after 100% relative reflection had been observed in the visible spectrum. The blood bag was gently shaken to provide homogeneity of the optical path. Without breaking the cold chain, color parameters were rapidly recorded in the computer.

4.5 Harboe Direct Spectrophotometric Technique

Hemolysis index can be determined by several techniques, Harboe technique has been considered to be the most accurate method [110]. In Harboe technique 3-point Allen correction was incorporated into the formula in order to measure only concentration of oxyhemoglobin and remove the significant effect of absorbance of other plasma

components such as albumin/bilirubin complexes and lipids. On the 7^{th}, 14^{th}, 21^{st}, 28^{th}, 35^{th}, 42^{nd} days of the storage, 5 ml of blood aseptically was drawn into vacuum tube and centrifuged at 3000 g for 10 minutes. The suspending medium was collected and diluted to 1/100 with distilled water. 200 μl samples from diluted sample were pipetted into a 96-well microplates. Absorbance of the samples on the well was read at 3 wavelengths (380, 415 and 450 nm) by microplate spectrophotometer. Absorbance quantities of all well were averaged. Plasma hemoglobin (g/dl) was calculated from the following formula.

$$Hb\,(g/dl) = (167.2 \times A_{415} - 83.6 \times A_{380} - 83.6 \times A_{450}) \times 1/1000 \times 1/dilution\,in\,water \tag{4.1}$$

The hemolysis index was finally observed by adding a hematocrit correction factor to the formula 4.2.

$$\%\,Hemolysis = \frac{Supernatant\,Hb \times (100 - Hct)}{Total\,Hb} \tag{4.2}$$

The total hemoglobin and the hematocrit values are those obtained from complete blood count, on the 0^{th} day.

5. RESULTS

24 color parameters were analyzed on daily basis during storage of 7 RBC concentrates. These parameters were tristimulus values X, Y, Z and chromaticity coordinates x, y, z, colorimetric purity and dominant wavelength of CIE 1931 XYZ system; chromaticity coordinates u, v of 1960 Yuv system; tristimulus values u', v', w', chromaticity coordinates u-v saturation and u-v hue angle of CIE 1964 U'V'W' space; axis Hunter L, Hunter a, Hunter b of Hunter Lab space; axis CIE L*, CIE a*, CIE b*, and other parameters CIELAB chroma, CIELAB hue angle of CIE L*a*b* space; and independent parameter correlated color temperature. These parameters are listed in (Table 5.1)

Color values of all RBC concentrates changed throughout the weeks, but only 8 of these color parameters showed statistically significant ($p<0.05$) changes for each sample (Table 5.1). As seen in the Table 5.1, during the first 3 weeks of storage none of the parameters changed significantly. After the 3^{rd} week of storage, tristimulus X and CIELAB chroma; after 4^{th} week u', u-v saturation, CCT, CIE a*, Hunter a and CIE 1960 u began to change significantly and the significance of the alterations increased in the following weeks. Since u' and CIE 1960 u are the same parameter, 7 colorimetric parameters (X, u', u-v saturation, CCT, Hunter a, CIE a*, CIELAB chroma) were further analyzed to search their relation with the degree of hemolysis.

Each week of storage, hemolysis of 7 samples were measured by Harboe spectrophotometric technique. The degree of hemolysis mean values of 7 samples and their standard deviations are illustrated in Figure 5.1.

Mean daily changes in 7 colorimetric parameters of all 7 RBC concentrates are illustrated in Figure 5.2 to Figure 5.8. Standard deviations in the changes of 7 samples, expression of the trend lines and the goodness of fits are also shown in these figures. According to these figures, tristimulus X, Hunter a and CIELAB chroma

Table 5.1
Statistical changes of colorimetric parameters through the weeks by considering each RBC concentrate separately. (*) corresponds to significance of the difference between the color values measured during 2^{nd}, 3^{rd}, 4^{th}, 5^{th} and 6^{th} weeks and measurement results of 1^{st} week. (*)=p<0.05, (**)=p<0.01, (***)=p<0.001.

	2^{nd} week	3^{rd} week	4^{th} week	5^{th} week	6^{th} week
X	-	-	*	*	**
Y	-	-	-	-	-
Z	-	-	-	-	-
x	-	-	*	-	-
y	-	-	-	-	-
z	-	-	-	-	-
Colorimetric purity	-	-	-	-	-
Dominant wavelength	-	-	-	-	-
CIE 1960 u	-	-	-	*	***
CIE 1960 v	-	-	-	-	-
u-v saturation	-	-	-	*	***
u-v hue angle	-	-	-	-	-
u'	-	-	-	*	***
v'	-	-	-	-	-
w'	-	-	*	-	-
Hunter L	-	-	-	-	-
Hunter a	-	-	-	**	***
Hunter b	-	-	-	-	-
CIE L*	-	-	-	-	-
CIE a*	-	-	-	**	***
CIE b*	-	-	-	-	-
CIELAB chroma	-	-	*	**	***
CIELAB hue angle	-	-	-	-	-
Color temperature	-	-	-	*	**

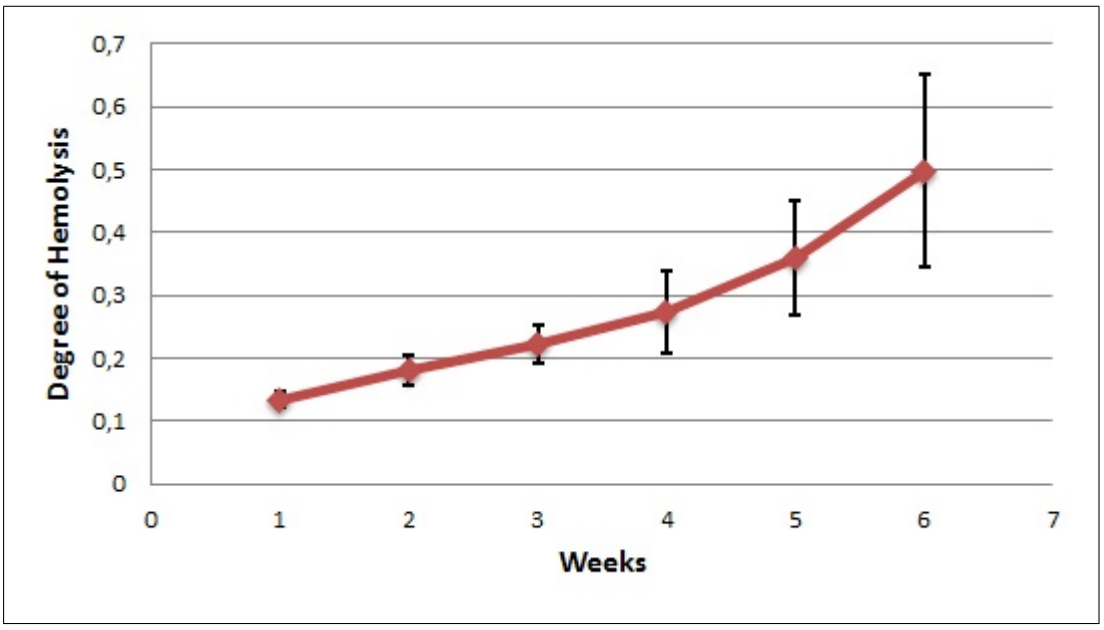

Figure 5.1 Weekly changes in the degree of hemolysis (7 samples).

linearly increased. Mean daily changes in the color coordinates: u', CIE a* and u-v saturation did not show a statistically significant change ($p<0.05$) for the first 14 days. After the 14^{th} day of storage, these parameters also increased linearly. However CCT exponentially decreased during storage period and saturated at about 1624 K. Since the hemolysis index does not have a limit, and progressively increases as storage continues, CCT can not be an indicator of hemolysis.

Sample wise standard deviations are slightly high, as seen in the previous graphs (Figure 5.2-5.8). Although slopes of the colorimetric parameters are very close in all the samples (Figure 5.9), 0^{th} day colorimetric values of the samples are different. Despite the fact that the hemolysis index of all RBC concentrates are expected to be zero in the first hours of blood collection, each RBC concentrate has an initial non-zero colorimetric value which differs from sample to sample. Consequently, a sample wise normalization was required. Based on these observations, normalization of samples is performed by dividing all measured values by their 0^{th} day values.

$$Normalized\,colorimetric\,value\,(n^{th}\,day) = \frac{Colorimetric\,value\,(n^{th}\,day)}{0^{th}\,day\,colorimetric\,value} \qquad (5.1)$$

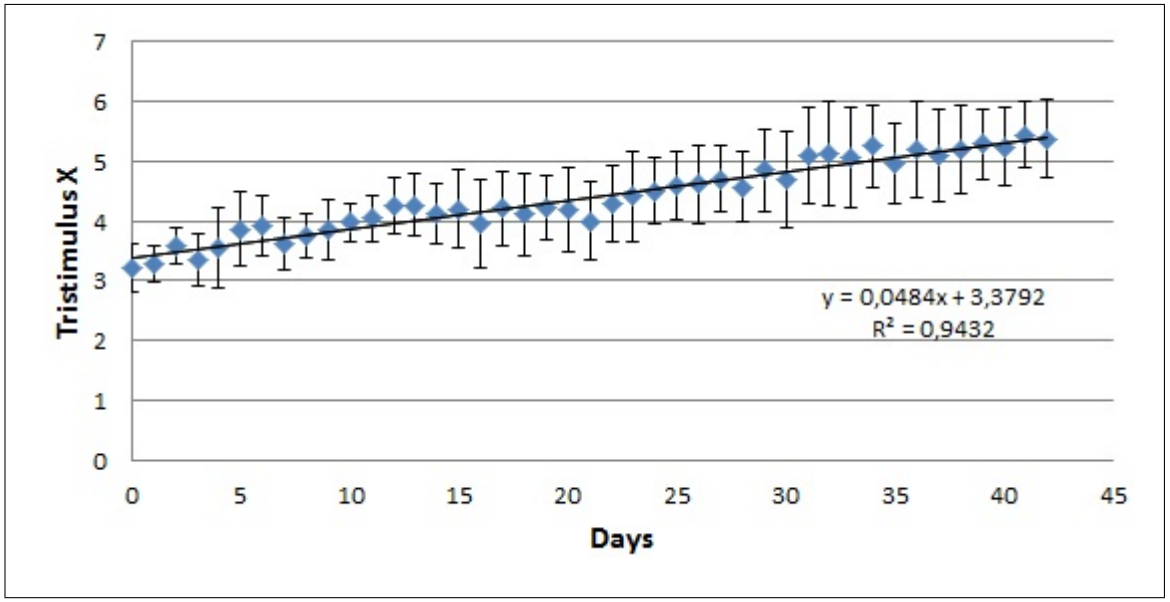

Figure 5.2 Daily changes in tristimulus value X (mean of 7 samples).

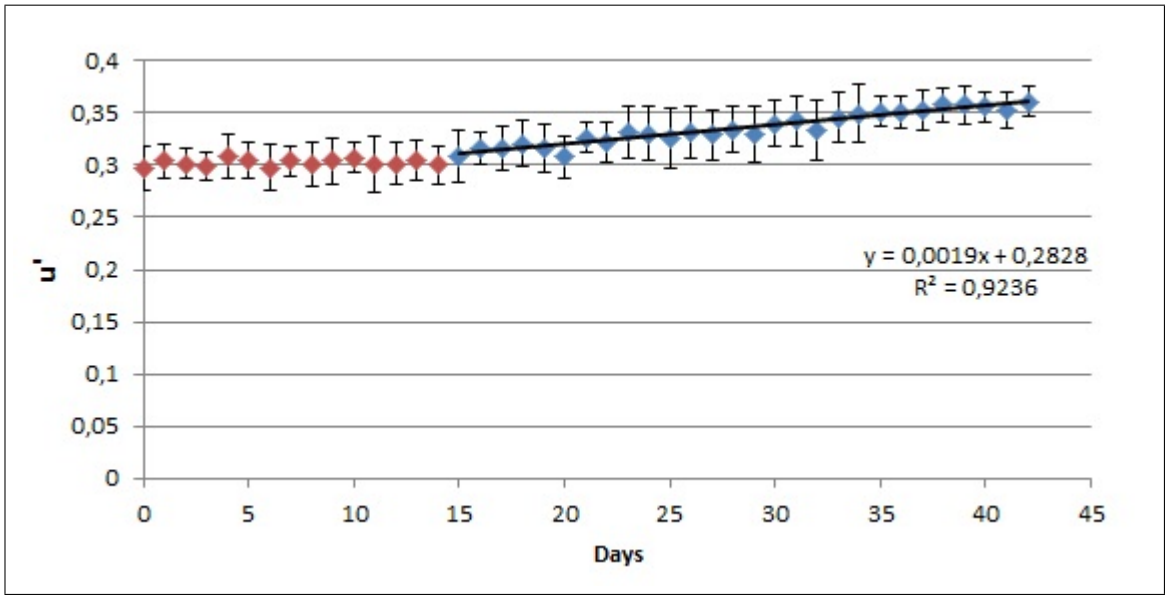

Figure 5.3 Daily changes in u' (mean of 7 samples). u' does not change significantly ($p<0.05$) until the 14^{th} day of the storage.

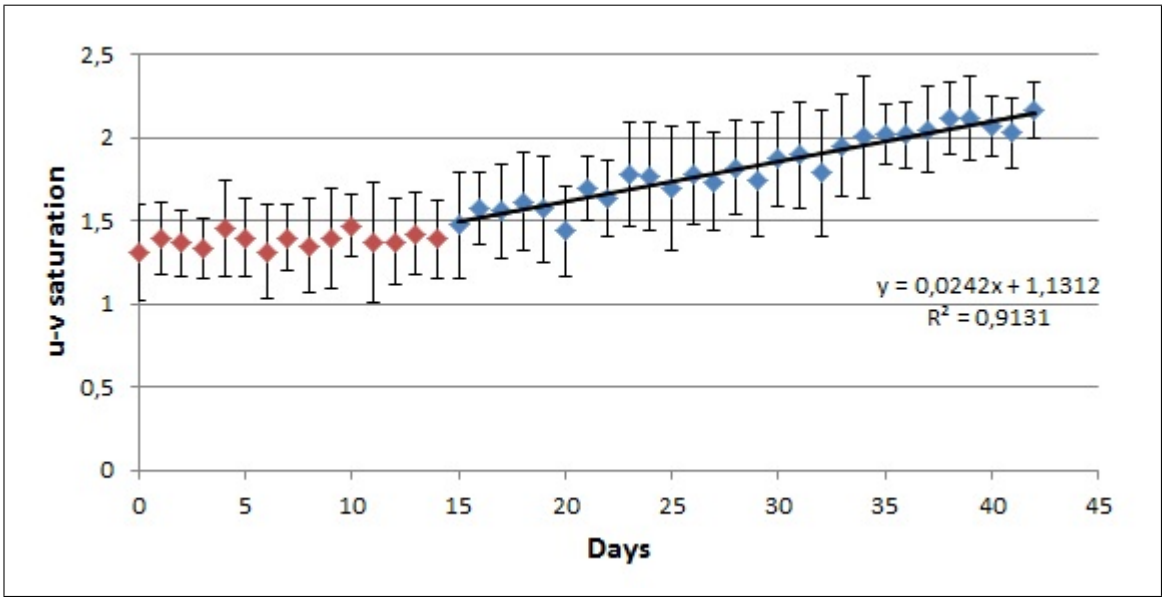

Figure 5.4 Daily changes in u-v saturation (mean of 7 samples). u-v saturation does not change significantly ($p<0.05$) until the 14^{th} day of the storage.

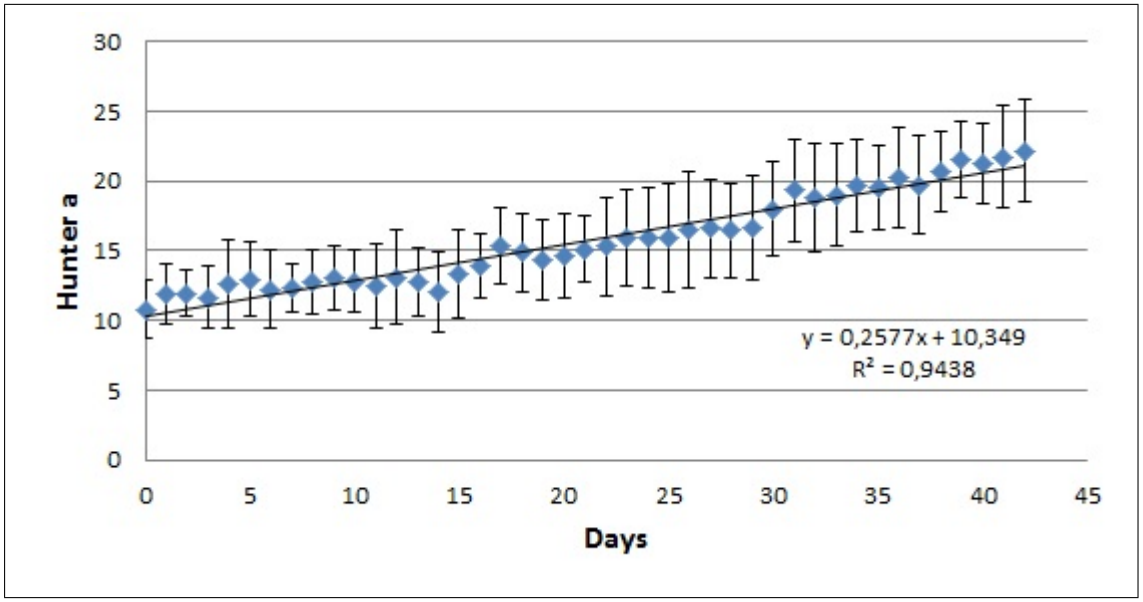

Figure 5.5 Daily changes in Hunter a (mean of 7 samples).

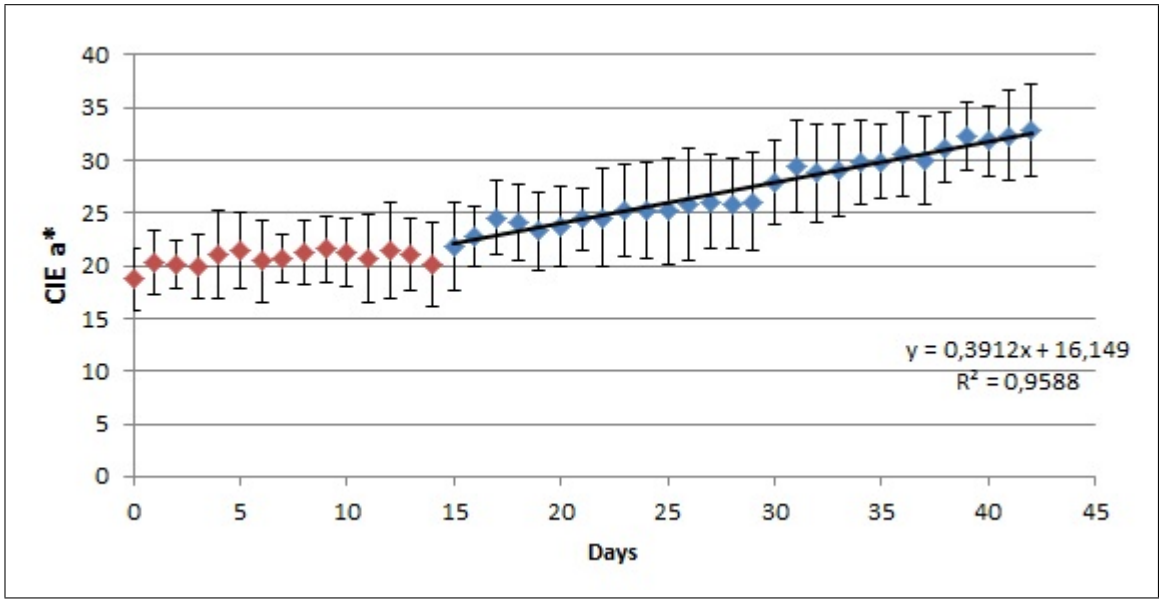

Figure 5.6 Daily changes in CIE a* (mean of 7 samples). CIE a* does not change significantly ($p<0.05$) until the 14^{th} day of the storage.

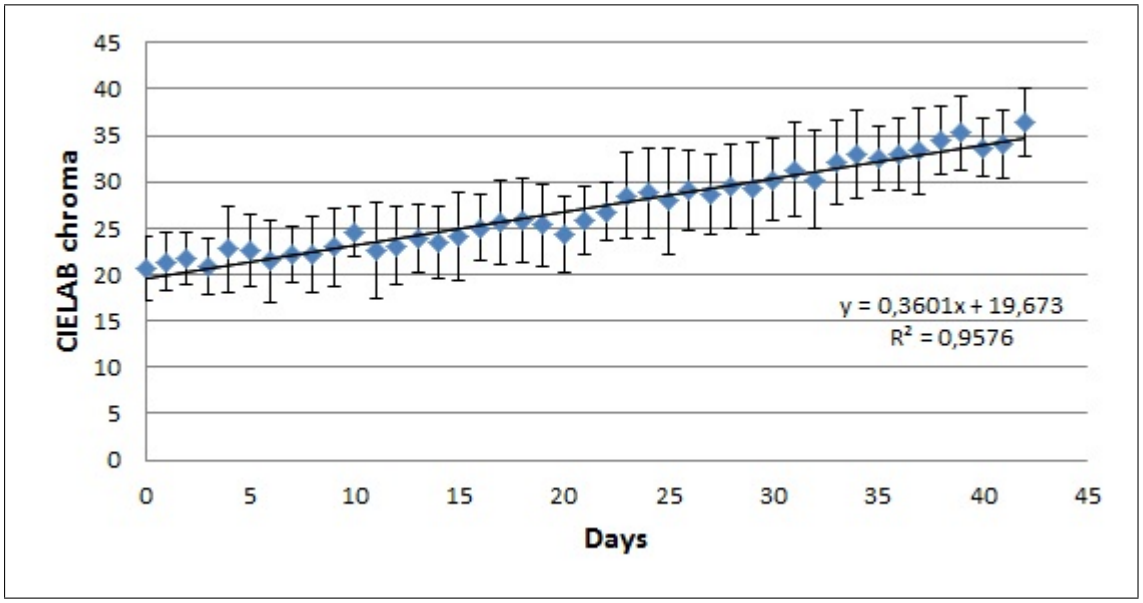

Figure 5.7 Daily changes in CIELAB chroma (mean of 7 samples).

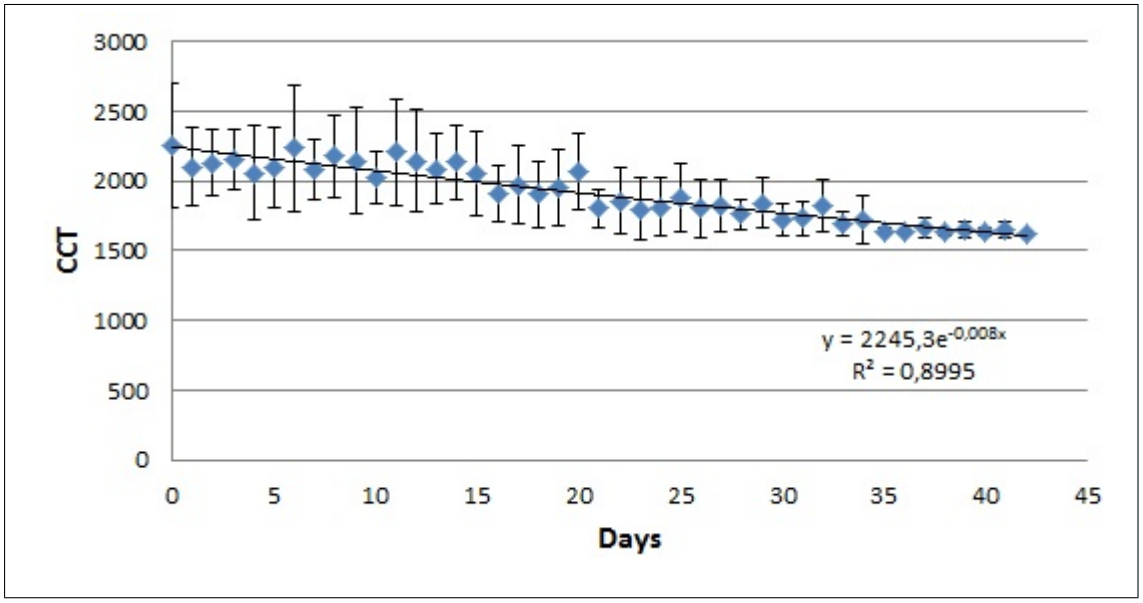

Figure 5.8 Daily changes in CCT (mean of 7 samples).

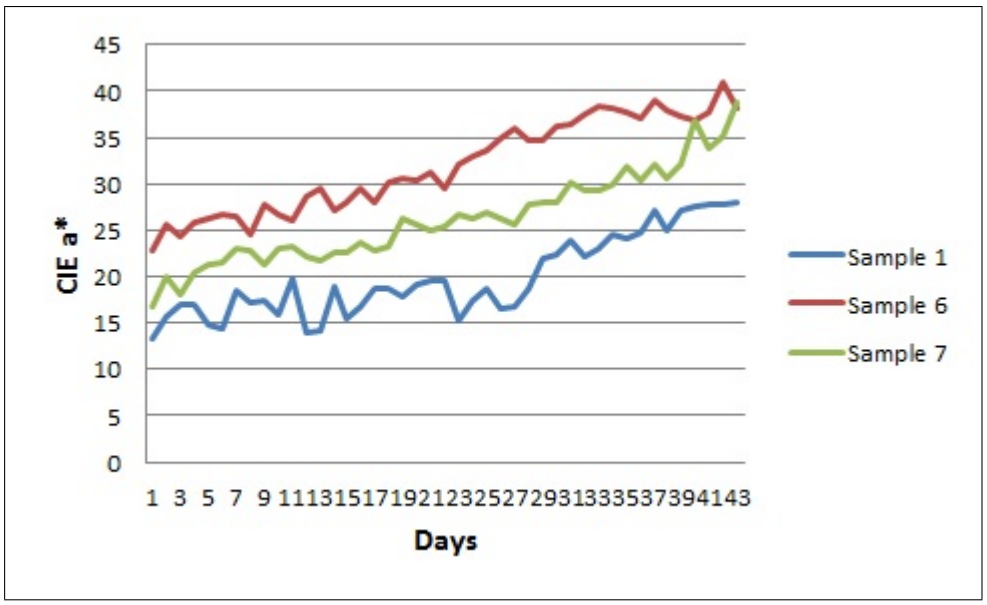

Figure 5.9 Sample wise difference in daily changes of CIE a*.

Table 5.2
Pearson's product correlation coefficient between colorimetric parameters and hemolysis index.

	Pearson's product correlation coefficient	p values
X	0.68	<0.005
u'	0.65	<0.005
u-v saturation	0.67	<0.005
CIE a*	0.71	<0.005
Hunter a	0.71	<0.005
CIELAB chroma	0.70	<0.005

Normalized colorimetric parameters can be a determining factor for the degree of hemolysis, if there is a correlation between hemolysis and any of these parameters. In order to investigate this correlation, for each sample, degrees of hemolysis and the normalized colorimetric value measured on the same day when the hemolysis measurements were performed are concatenated and a 42x6 (7 samples x 6 weeks x 6 normalized parameters) matrix was formed (Appendix B.1). Correlation between the normalized parameters and hemolysis index was calculated. Pearson's product correlation coefficients and their p-values are listed in Table 5.2. Scatter plots of hemolysis index versus normalized colorimetric parameters are illustrated in Appendix B (Figure B1-B6).

6. DISCUSSION

Color measurement technique is a safe and easy technique when compared to other techniques that use centrifugation or chemical reagents [111]. Although the instruments used in the experiments are robust, easy to handle, measurements with these instruments are time consuming because of the procedures such as waiting for the settlement of light source, taking reference measurements with white diffuse reflectance standard. There are commercially available one-piece colorimeters that make quick measurements. Another uncomfortability of the instruments is that the color measurement has to be performed in a dark room. Colorimeters using daylight provide more comfortable measurements. Practically, cameras can also be used in colorimetry with image processing techniques [112, 113, 114, 115]. However, due to the alterations in angle of application and in spectral energy distribution of the illuminant error rates increase in color cameras.

Colorimetric parameters that significantly changed during storage are related to the red content of the stimulus in the color spaces. Tristimulus X is calculated by convolving the relative reflection spectrum, with matching function $\overline{x}(\lambda)$ which correspond to spectral sensitivity function of ρ cone [116]. Coordinate values CIE a* and Hunter a refer to saturation of red when it is positive. Uniform chromaticity coordinate value u' mostly depends on tristimulus X. CCT become more reddish when it decrease below 2000 K as it was measured in experiments. Other colorimetric parameters that changed significantly during storage (u-v saturation and CIELAB chroma)correspond to the distance of any color stimulus from white point. Other colorimetric parameters, except these 7 colorimetric parameters, did not change significantly in any of the samples during storage ($p<0.05$) (Table 5.1).

Even though chromaticity coordinate values x and u' have the same role in different color spaces, daily changes in x did not change significantly as it is in u'. The reason for this is the non-uniformity of xy chromaticity diagram and uniformity of u'-v'

chromaticity diagram. Similarly, colorimetric purity in xy chromaticity diagram did not change significantly during storage, in contrast u-v saturation in u'-v' chromaticity diagram and CIELAB chroma in CIE L*a*b* space. Uniformity is a property of a color space where equal distances on the coordinate diagram correspond to equal perceived color differences. As a result, it is important to choose uniform color spaces in analyzing hemolysis.

When analyzing the colorimetric parameters of the samples, the colorimetric parameters of at least one sample did not change significantly ($p<0.05$). However, when all samples were examined together, mean daily changes of parameters became linear as illustrated in Figure 5.2 to 5.8. Mean daily changes in tristimulus X, Hunter a, CIELAB chroma were linearly fitted and goodness of fits, R^2 were 0.94, 0.94, 0.96, respectively. On the other hand, u', u-v saturation, CIE a* did not significantly change until the 14^{th} day of storage. That means these parameters were not sensitive to any physiological or morphological changes inside the blood bag for the first 2 weeks of storage. After the 2^{nd} week of storage, u', u-v saturation, CIE a* also showed a linear increase with R^2 values 0.92, 0.91, 0.96 respectively. Changes in these parameters satisfy studies that emphasize the 14^{th} day of storage when physiological and morphological alterations in red cells become critical [74, 117]. CCT showed an exponential decrease during storage and converged to 1624 K. Since hemolysis does not converge to any degree, CCT was not analyzed in correlation analysis.

Hemolysis index generally shows a low-rate linear increase during first weeks and exponentially increases after 3^{rd} week of storage [4, 6, 36, 38, 118]. Hemolysis measurements obtained from Harboe spectrophotometric technique which was performed each week of storage reveal similar results with the literature (Figure 5.1). Results also prove the high standard deviations of donors in degree of hemolysis [4, 29, 36, 39, 118]. Since, according to Figure 5.1, the average degree of hemolysis in the first 3 weeks is very low ($0.22\%\pm0.03\%$) and far below the acceptable level; it is not necessary to determine hemolysis for first 3 weeks. However, standard deviations of blood samples from different donors start to increase (0.06%-0.15%) after the 3^{rd} week of storage, so determination of hemolysis become significant. This clarifies the results in Table 5.1

that all colorimetric parameters of each sample do not significantly ($p<0.05$) change in the first 3 weeks.

The colorimetric difference of RBC concentrates at the 0^{th} day were visually observable. Some of the samples were nearly black in color, while some others were lighter red. For example, tristimulus X value of the blackish red unit was measured around 2.5 to 2.7; lighter red ones were measured at 0^{th} day around 3.2 to 3.5. Average standard deviations of colorimetric parameters were very high, for instance it was 0.60 for tristimulus X. Since the hemolysis index in the 0^{th} day is expected to be 0, in order to relate the degree of hemolysis and colorimetric parameters, colorimetric parameters are need to be normalized. Normalization was performed by dividing all values by the 0^{th} day value. This is the disadvantage of the colorimetric method to measure hemolysis because all results depend on the 0^{th} day data.

Changes in normalized tristimulus X, u', u-v saturation, CIE a*, CIELAB chroma, Hunter a satisfy the changes in hemolysis. According to the correlation analysis between those parameters and the hemolysis index, CIE a* and Hunter a have stronger correlation ($r=0.71$) with hemolysis than others. Even though, Pearson's product correlation coefficients of all parameters are very close to each other. CIE a*, Hunter a, CIELAB chroma have strong correlation with the hemolysis ($r>0.70$), tristimulus X, u', u-v saturation have moderate correlation ($0.4<r<0.7$).

Currently there is a need for a sensor for the assessment of the quality of blood bags, without opening the bag. Plasma hemoglobin concentration serves as an indicator for the hemolysis, but plasma hemoglobin can not be measured accurately without centrifugation. A non-invasive plasma hemoglobin measurement device performing measurement from the tube connected to blood bag by analyzing reflected light at two wavelengths (560 nm and 700 nm), was introduced and a precision of 1.6% was declared [87]. However, the disadvantage of this technique was that sedimentation of erythrocytes was required, before measurement. In a different related study on measuring the hemolysis without centrifugation, Bermakai *et al.* concluded that there is a correlation between the degree of hemolysis and the percentage of light transmittance

at the wavelengths between 410 and 480 nm [10]. In this study, correlation between the degree of hemolysis and reflectance of light at visible spectrum was confirmed, but changes in reflectance were in the wavelength region near 600 nm.

7. CONCLUSION

Quality determination of stored blood is essential for minimizing transfusion related adverse outcomes. Visual assessment of hemolysis is used to estimate quality of blood products by inspecting change in color of suspending media. Changes in color of suspending media definitely result in color change in whole blood which is the motivation of the study. The most accurate way of measuring the color of a sample, is by specifying the visual stimulus reflected from the sample, in a three dimensional color system instead of comparing with colored charts. In this study, both standard hemolysis measurements and color measurements were performed and 24 colorimetric parameters in various color spaces (CIE XYZ, U'V'W', Yuv, L*a*b*, Hunter Lab) were analyzed during 42 days of storage period.

As a result, 3 normalized colorimetric parameters which are Hunter a, CIE a* and CIELAB chroma showed strong correlations with the degree of hemolysis. Although, CIE a* and Hunter a are the most correlated parameters ($r=0.71$) ($p<0.005$), Hunter a is more suitable for determining degree of hemolysis, since CIE a* is not sensitive enough in the first 2 weeks (Figure 5.6). In conclusion, determination of hemolysis with a non-invasive color measurement can be possible in the future. Safe and quick analysis of blood quality would be an important improvement in transfusion medicine.

APPENDIX A. Tables for the Color Calculations

Table A.1
Color matching functions of 2^0 observer [96].

λ(nm)	$\overline{x}(\lambda)$	$\overline{y}(\lambda)$	$\overline{z}(\lambda)$	λ(nm)	$\overline{x}(\lambda)$	$\overline{y}(\lambda)$	$\overline{z}(\lambda)$
380	0.0014	0.0000	0.0065	580	0.9163	0.8700	0.0017
385	0.0022	0.0001	0.0105	585	0.9786	0.8163	0.0014
390	0.0042	0.0001	0.0201	590	1.0263	0.7570	0.0011
395	0.0076	0.0002	0.0362	595	1.0567	0.6949	0.0010
400	0.0143	0.0004	0.0679	600	1.0622	0.6310	0.0008
405	0.0232	0.0006	0.1102	605	1.0456	0.5668	0.0006
410	0.0435	0.0012	0.2074	610	1.0026	0.5030	0.0003
415	0.0776	0.0022	0.3713	615	0.9384	0.4412	0.0002
420	0.1344	0.0040	0.6456	620	0.8544	0.3810	0.0002
425	0.2148	0.0073	1.0391	625	0.7514	0.3210	0.0001
430	0.2839	0.0116	1.3856	630	0.6424	0.2650	0.0000
435	0.3285	0.0168	1.6230	635	0.5419	0.2170	0.0000
440	0.3483	0.0230	1.7471	640	0.4479	0.1750	0.0000
445	0.3481	0.0298	1.7826	645	0.3608	0.1382	0.0000
450	0.3362	0.0380	1.7721	650	0.2835	0.1070	0.0000
455	0.3187	0.0480	1.7441	655	0.2187	0.0816	0.0000
460	0.2908	0.0600	1.6692	660	0.1649	0.0610	0.0000
465	0.2511	0.0739	1.5281	665	0.1212	0.0446	0.0000
470	0.1954	0.0910	1.2876	670	0.0874	0.0320	0.0000
475	0.1421	0.1126	1.0419	675	0.0636	0.0232	0.0000
480	0.0956	0.1390	0.8130	680	0.0468	0.0170	0.0000
485	0.0580	0.1693	0.6162	685	0.0329	0.0119	0.0000
490	0.0320	0.2080	0.4652	690	0.0227	0.0082	0.0000
495	0.0147	0.2586	0.3533	695	0.0158	0.0057	0.0000
500	0.0049	0.3230	0.2720	700	0.0114	0.0041	0.0000
505	0.0024	0.4073	0.2123	705	0.0081	0.0029	0.0000
510	0.0093	0.5030	0.1582	710	0.0058	0.0021	0.0000
515	0.0291	0.6082	0.1117	715	0.0041	0.0015	0.0000
520	0.0633	0.7100	0.0782	720	0.0029	0.0010	0.0000
525	0.1096	0.7932	0.0573	725	0.0020	0.0007	0.0000
530	0.1655	0.8620	0.0422	730	0.0014	0.0005	0.0000
535	0.2257	0.9149	0.0298	735	0.0010	0.0004	0.0000
540	0.2904	0.9540	0.0203	740	0.0007	0.0003	0.0000
545	0.3597	0.9803	0.0134	745	0.0005	0.0002	0.0000
550	0.4334	0.9950	0.0087	750	0.0003	0.0001	0.0000
555	0.5121	1.0002	0.0057	755	0.0002	0.0001	0.0000
560	0.5945	0.9950	0.0039	760	0.0002	0.0001	0.0000
565	0.6784	0.9786	0.0027	765	0.0001	0.0000	0.0000
570	0.7621	0.9520	0.0021	770	0.0001	0.0000	0.0000
575	0.8425	0.9154	0.0018	775	0.0000	0.0000	0.0000
				Totals	21.37	21.37	21.37

Table A.2
Coordinates of white point of illuminant D_{65} [104].

X	Y	Z	x	y	u'	v'
95.04	100.00	108.89	0.3127	0.3290	0.1978	0.4683

Table A.3
Relative spectral power distribution of CIE Standard Illuminant D_{65} [88].

λ(nm)	D_{65}	λ(nm)	D_{65}	λ(nm)	D_{65}	λ(nm)	D_{65}
300	0.0341	435	95.7736	570	96.3342	705	72.9790
305	1.6643	440	104.865	575	96.0611	710	74.3490
310	3.2945	445	110.936	580	95.7880	715	67.9765
315	11.7652	450	117.008	585	92.2368	720	61.6040
320	20.2360	455	117.410	590	88.6856	725	65.7448
325	28.6447	460	117.812	595	89.3459	730	69.8856
330	37.0535	465	116.337	600	90.0062	735	72.4863
335	38.5011	470	114.861	605	89.8026	740	75.0870
340	39.9488	475	115.392	610	89.5991	745	69.3398
345	42.4302	480	115.923	615	88.6489	750	63.5927
350	44.9117	485	112.367	620	87.6987	755	55.0054
355	45.7750	490	108.811	625	85.4936	760	46.4182
360	46.6383	495	109.083	630	83.2886	765	56.6118
365	49.3637	500	109.354	635	83.4939	770	66.8054
370	52.0891	505	108.578	640	83.6992	775	65.0941
375	51.0323	510	107.802	645	81.8630	780	63.3828
380	49.9755	515	106.296	650	80.0268	785	63.8434
385	52.3118	520	104.790	655	80.1207	790	64.3040
390	54.6482	525	106.240	660	80.2146	795	61.8779
395	68.7015	530	107.689	665	81.2462	800	59.4519
400	82.7549	535	106.047	670	82.2778	805	55.7054
405	87.1204	540	104.405	675	80.2810	810	51.9590
410	91.4860	545	104.226	680	78.2842	815	54.6998
415	92.4589	550	104.046	685	74.0027	820	57.4406
420	93.4318	555	102.023	690	69.7213	825	58.8765
425	90.0570	560	100.000	695	70.6652	830	60.3125
430	86.6823	565	98.1671	700	71.6091		

Table A.4
Chromaticity coordinates of spectrum locus [104].

λ(nm)	$\overline{x}(\lambda)$	$\overline{y}(\lambda)$	u'(λ)	v'(λ)	λ(nm)	$\overline{x}(\lambda)$	$\overline{y}(\lambda)$	u'(λ)	v'(λ)
380	0.1741	0.0050	0.2569	0.0165	585	0.5448	0.4544	0.2959	0.5554
385	0.1740	0.0050	0.2567	0.0165	590	0.5752	0.4242	0.3315	0.5501
390	0.1738	0.0049	0.2564	0.0163	595	0.6029	0.3965	0.3681	0.5446
395	0.1736	0.0049	0.2560	0.0163	600	0.6270	0.3725	0.4035	0.5393
400	0.1733	0.0048	0.2558	0.0159	605	0.6482	0.3514	0.4380	0.5342
405	0.1730	0.0048	0.2553	0.0159	610	0.6658	0.3340	0.4691	0.5296
410	0.1726	0.0048	0.2545	0.0159	615	0.6801	0.3197	0.4967	0.5254
415	0.1721	0.0048	0.2537	0.0160	620	0.6915	0.3083	0.5202	0.5219
420	0.1714	0.0051	0.2522	0.0169	625	0.7006	0.2993	0.5399	0.5190
425	0.1703	0.0058	0.2496	0.0191	630	0.7079	0.2920	0.5565	0.5165
430	0.1689	0.0069	0.2461	0.0226	635	0.7140	0.2859	0.5709	0.5144
435	0.1669	0.0086	0.2411	0.0278	640	0.7190	0.2809	0.5830	0.5125
440	0.1644	0.0109	0.2347	0.0349	645	0.7230	0.2770	0.5930	0.5110
445	0.1611	0.0138	0.2267	0.0437	650	0.7260	0.2740	0.6005	0.5099
450	0.1566	0.0177	0.2161	0.0550	655	0.7283	0.2717	0.6064	0.5090
455	0.1510	0.0227	0.2033	0.0689	660	0.7300	0.2700	0.6108	0.5084
460	0.1440	0.0297	0.1877	0.0871	665	0.7311	0.2689	0.6138	0.5079
465	0.1355	0.0399	0.1690	0.1119	670	0.7320	0.2680	0.6161	0.5076
470	0.1241	0.0578	0.1441	0.1510	675	0.7327	0.2673	0.6181	0.5073
475	0.1096	0.0868	0.1147	0.2044	680	0.7334	0.2666	0.6200	0.5070
480	0.0913	0.1327	0.0828	0.2708	685	0.7340	0.2660	0.6216	0.5068
485	0.0687	0.2007	0.0521	0.3427	690	0.7344	0.2656	0.6226	0.5066
490	0.0454	0.2950	0.0282	0.4117	695	0.7346	0.2654	0.6231	0.5065
495	0.0235	0.4127	0.0119	0.4698	700	0.7347	0.2653	0.6234	0.5065
500	0.0082	0.5384	0.0035	0.5131	705	0.7347	0.2653	0.6234	0.5065
505	0.0039	0.6548	0.0014	0.5432	710	0.7347	0.2653	0.6234	0.5065
510	0.0139	0.7502	0.0046	0.5638	715	0.7347	0.2653	0.6234	0.5065
515	0.0389	0.8120	0.0123	0.5770	720	0.7347	0.2653	0.6234	0.5065
520	0.0743	0.8338	0.0231	0.5837	725	0.7347	0.2653	0.6234	0.5065
525	0.1142	0.8262	0.0360	0.5861	730	0.7347	0.2653	0.6234	0.5065
530	0.1547	0.8059	0.0501	0.5868	735	0.7347	0.2653	0.6234	0.5065
535	0.1929	0.7816	0.0643	0.5865	740	0.7347	0.2653	0.6234	0.5065
540	0.2296	0.7543	0.0792	0.5856	745	0.7347	0.2653	0.6234	0.5065
545	0.2658	0.7243	0.0953	0.5841	750	0.7347	0.2653	0.6234	0.5065
550	0.3016	0.6923	0.1127	0.5821	755	0.7347	0.2653	0.6234	0.5065
555	0.3373	0.6589	0.1319	0.5796	760	0.7347	0.2653	0.6234	0.5065
560	0.3731	0.6245	0.1531	0.5766	765	0.7347	0.2653	0.6234	0.5065
565	0.4087	0.5896	0.1766	0.5732	770	0.7347	0.2653	0.6234	0.5065
570	0.4441	0.5547	0.2026	0.5694	775	0.7347	0.2653	0.6234	0.5065
575	0.4788	0.5202	0.2312	0.5651	780	0.7347	0.2653	0.6234	0.5065
580	0.5125	0.4866	0.2623	0.5604					

APPENDIX B. Additional Illustrations of Results

Table B.1
Weekly results of Samples.

		X	u'	u-v ha	Hun a	CIE a	chroma
Sample 1	1^{st} week	1.194	1.048	1.013	1.178	1.135	1.128
	2^{nd} week	1.076	1.062	1.068	1.109	1.090	1.120
	3^{rd} week	1.151	1.090	1.189	1.202	1.162	1.292
	4^{th} week	1.481	1.118	1.265	1.469	1.346	1.448
	5^{th} week	1.514	1.228	1.607	1.868	1.643	1.733
	6^{th} week	1.668	1.259	1.699	2.078	1.786	1.863
Sample 2	1^{st} week	1.108	1.017	0.996	1.103	1.079	1.073
	2^{nd} week	1.284	1.048	1.083	1.267	1.195	1.199
	3^{rd} week	1.061	1.126	1.295	1.362	1.295	1.293
	4^{th} week	1.403	1.077	1.201	1.276	1.195	1.372
	5^{th} week	1.427	1.155	1.372	1.698	1.520	1.495
	6^{th} week	1.464	1.206	1.522	1.790	1.584	1.643
Sample 3	1^{st} week	1.047	1.014	1.023	1.104	1.059	1.062
	2^{nd} week	1.109	1.018	1.035	1.138	1.080	1.089
	3^{rd} week	1.241	1.097	1.277	1.419	1.292	1.238
	4^{th} week	1.320	1.115	1.356	1.446	1.304	1.437
	5^{th} week	1.568	1.160	1.480	1.737	1.500	1.595
	6^{th} week	1.667	1.255	1.761	2.125	1.769	1.856
Sample 4	1^{st} week	1.130	1.025	1.068	1.200	1.152	1.139
	2^{nd} week	1.309	1.031	1.140	1.098	1.054	1.265
	3^{rd} week	1.309	1.061	1.184	1.359	1.264	1.290
	4^{th} week	1.328	1.091	1.269	1.483	1.359	1.366
	5^{th} week	1.406	1.140	1.430	1.587	1.433	1.519
	6^{th} week	1.520	1.146	1.442	1.698	1.507	1.569
Sample 5	1^{st} week	1.048	0.970	0.903	1.078	1.052	0.971
	2^{nd} week	1.315	0.988	1.006	1.040	1.003	1.122
	3^{rd} week	1.273	1.091	1.274	1.421	1.310	1.313
	4^{th} week	1.374	1.093	1.279	1.505	1.365	1.355
	5^{th} week	1.531	1.158	1.477	1.738	1.531	1.572
	6^{th} week	1.665	1.173	1.514	1.888	1.627	1.641
Sample 6	1^{st} week	1.091	0.983	0.991	1.079	1.082	1.051
	2^{nd} week	1.204	1.024	1.098	1.197	1.174	1.165
	3^{rd} week	1.339	1.055	1.175	1.364	1.296	1.284
	4^{th} week	1.431	1.143	1.396	1.599	1.473	1.475
	5^{th} week	1.611	1.151	1.410	1.741	1.567	1.535
	6^{th} week	1.572	1.132	1.352	1.789	1.604	1.490
Sample 7	1^{st} week	1.162	1.034	1.078	1.125	1.093	1.123
	2^{nd} week	1.179	1.032	1.070	1.119	1.086	1.113
	3^{rd} week	1.283	1.083	1.126	1.317	1.236	1.266
	4^{th} week	1.361	1.109	1.277	1.439	1.327	1.336
	5^{th} week	1.538	1.172	1.453	1.683	1.499	1.532
	6^{th} week	1.621	1.158	1.414	1.994	1.720	1.623

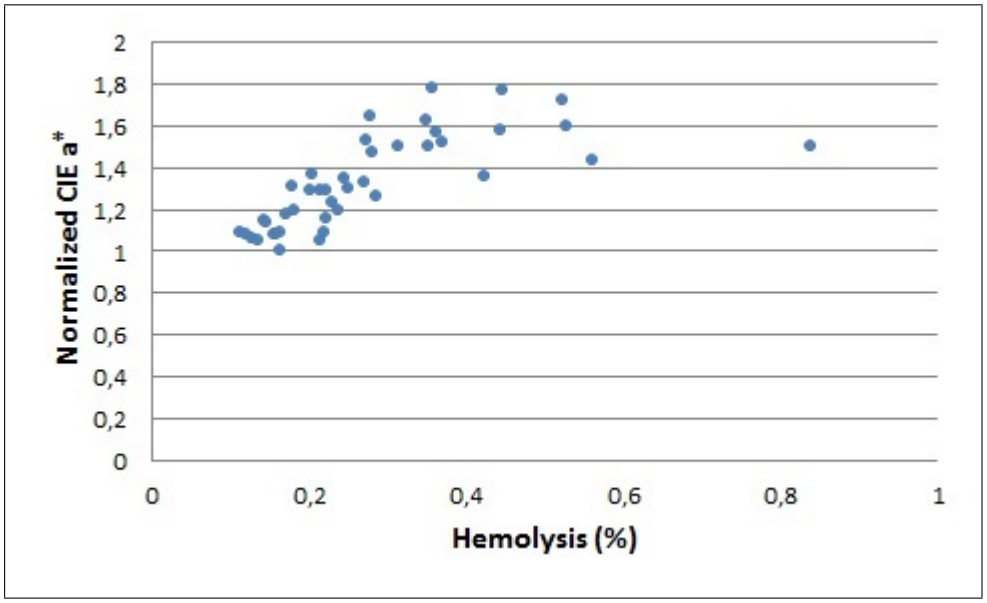

Figure B.1 Normalized CIE a* versus degree of hemolysis.

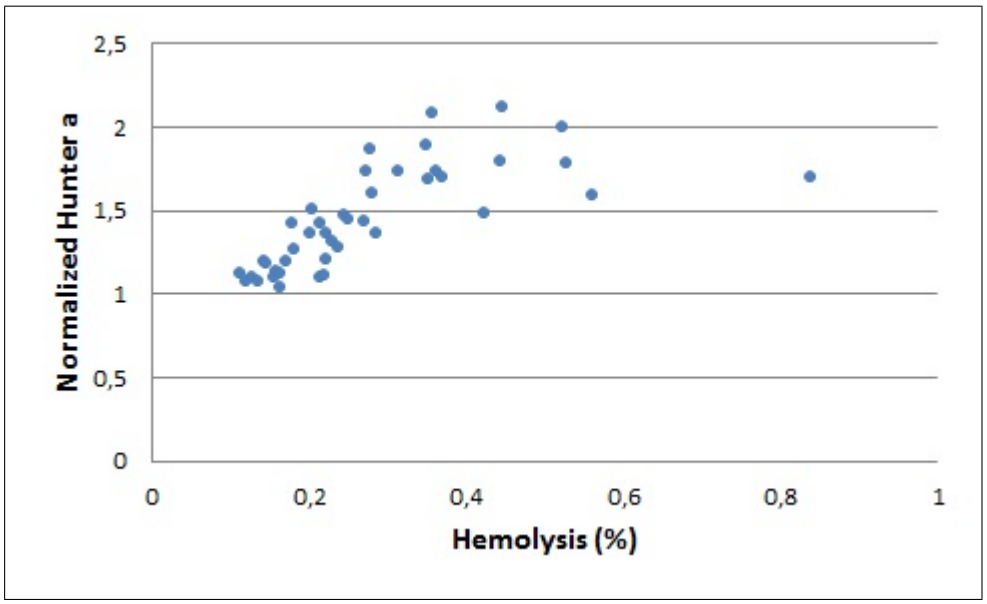

Figure B.2 Normalized Hunter a versus degree of hemolysis.

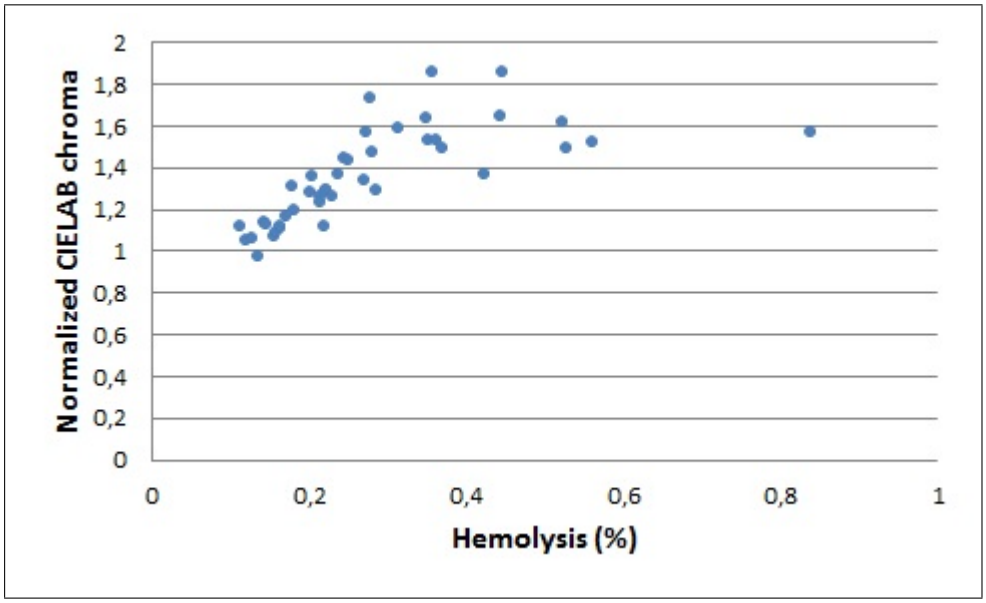

Figure B.3 Normalized CIELAB chroma versus degree of hemolysis.

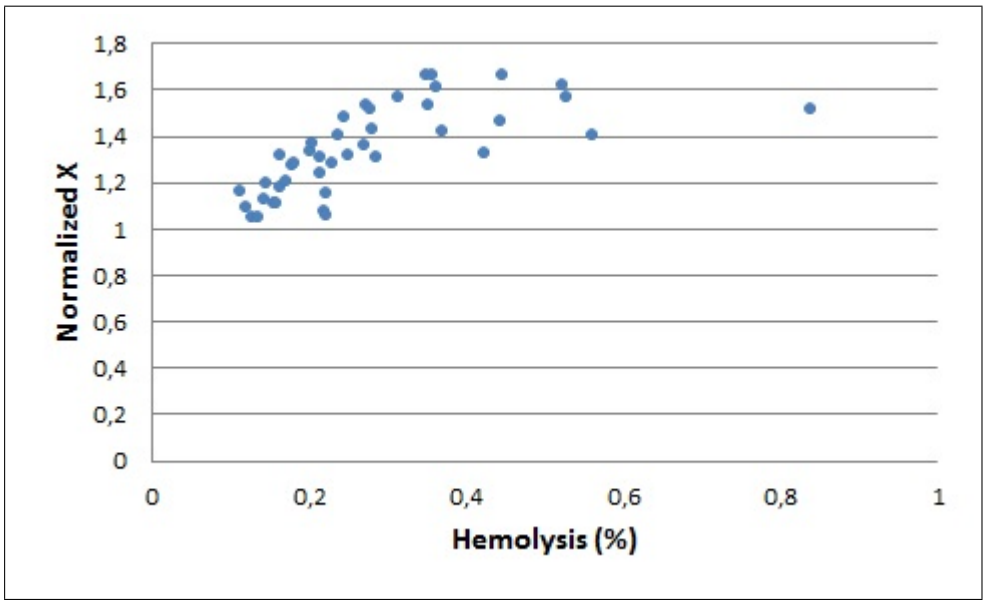

Figure B.4 Normalized X versus degree of hemolysis.

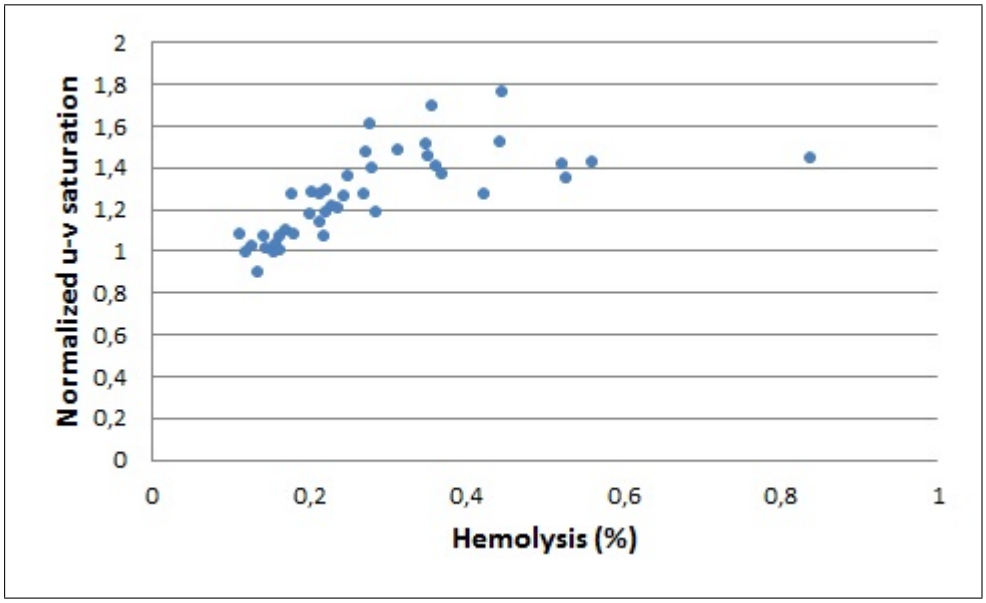

Figure B.5 Normalized u-v saturation versus degree of hemolysis.

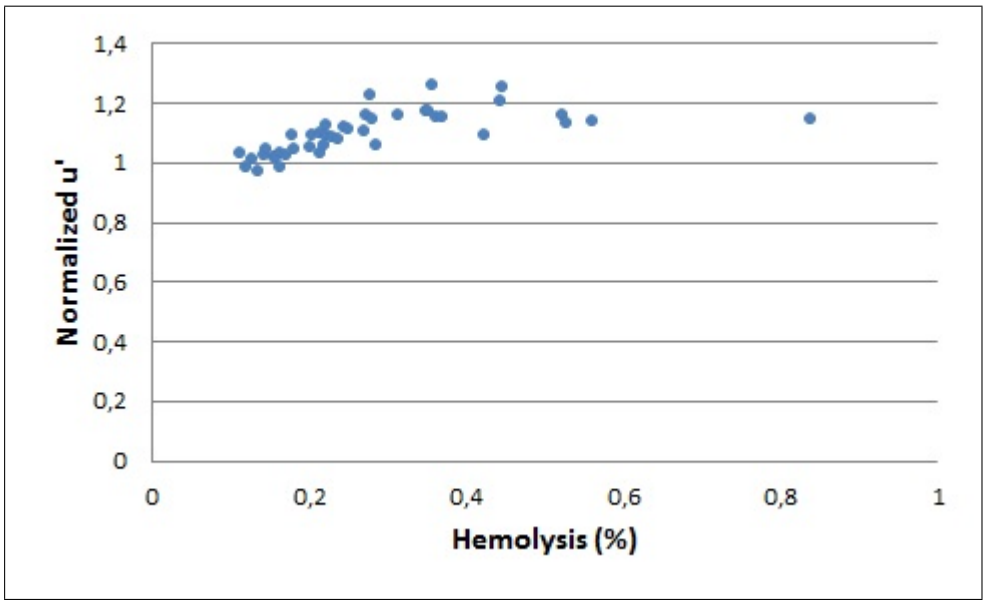

Figure B.6 Normalized u versus degree of hemolysis.

REFERENCES

1. Triulzi, D. J., and M. H. Yazer, "Clinical studies of the effect of blood storage on patient outcomes," *Transfusion and Apheresis Science*, Vol. 43, pp. 95–106, Aug 2010.

2. Can, O. M., Y. Ülgen, and H. Bilgen, "Monitoring Cole parameters of red blood cell concentrates during storage," *Abstract Book of International Workshop on Impedance Spectroscopy*, Vol. 6, p. 96, Sep 2013.

3. Janatpour, K. A., T. G. Paglieroni, V. L. Crocker, D. J. DuBois, and P. V. Holland, "Visual assessment of hemolysis in red blood cell units and segments can be deceptive," *Transfusion*, Vol. 44, pp. 984–989, July 2004.

4. Sowemimo-Coker, S. O., "Red blood cells hemolysis during processing," *Transfusion Medicine Reviews*, Vol. 16, pp. 46–60, Jan 2002.

5. Segatchian, J., P. Krailadsiri, M. Beard, and M. Vickers, "Development of a microplate method for the measurement of plasma haemoglobin and its use in monitoring the storage lesion of red cell component," *Transfusion and Apheresis Science*, Vol. 26, pp. 91–93, Feb 2002.

6. Gandhi, M. J., E. Shapiro, L. Emmert, D. M. Strong, and T. H. Price, "Prestorage leukoreduction does not increase hemolysis of stored red cell concentrates," *Transfusion and Apheresis Science*, Vol. 36, pp. 17–22, Jan 2007.

7. "Visual assessment guide," tech. rep., Canadian Blood Services, Jan 2009.

8. Meinke, M., I. Gersonde, M. Friebel, J. Helfmann, and G. Müller, "Chemometric determination of blood parameters using visible-near-infrared spectra," *Applied Spectroscopy*, Vol. 59, pp. 826–835, June 2005.

9. Neudel, F., *Erfassung der Hämolyse mittels optischer Reflexionsspektroskopie*. PhD thesis, RWTH Aachen, Aachen, Germany, 2002.

10. Bermakai, M. Y., M. S. Jaafar, A. L. Ahmad, N. E. Ismail, and N. Zakariyah, "Study on hemolysis in whole-blood sample due to longer storage by visible light irradiation," *Proceedings of the 3^{rd} Asian Physics Symposium*, pp. 365–369, July 2009.

11. Sparrow, R. L., "Red blood cell storage and transfusion-related immunomodulation," *Blood Transfusion*, Vol. 8, pp. s26–s30, June 2010.

12. Cantürk, E., S. Ceylan, U. Y. Akgün, A. Y. Kulular, Y. Kurtulus, A. Alnawajha, M. Sengelen, and D. Aslan, "Does volunteerism make any difference to admissions to blood centers: An evaluation from admissions to two selected blood centers in Ankara," *Turkish Journal of Public Health*, Vol. 11, no. 2, pp. 86–95, 2013.

13. Greening, D. W., K. M. Glenister, R. L. Sparrow, and R. J. Simpson, "International blood collection and storage: Clinical use of blood products," *Journal of Proteomics*, Vol. 73, no. 3, pp. 386–395, 2010.

14. Zolla, L., and A. D'Alessandro, "An efficeint apparatus for rapid deoxygenation of erythrocyte concentrates for alternative banking strategies," *Journal of Blood Transfusion*, Vol. 2013, Jan 2013.

15. D'Alessandro, A., G. Liumbruno, G. Grazzini, and L. Zolla, "Red blood cell storage: the story so far," *Blood Transfusion*, Vol. 8, pp. 82–88, Apr 2010.

16. "Ulusal kan ve kan ürünleri rehberi," tech. rep., Ministery of Health of Turkey, 2011.

17. "Guide to the preparation, use and quality assurance of blood components - 13th edition," tech. rep., European Council, 2007.

18. Hess, J. R., "Red cell storage," *Journal of Proteomics*, Vol. 73, pp. 368–373, Jan 2010.

19. Hess, J. R., "Red cell changes during storage," *Journal of Apheresis Sciences*, Vol. 43, pp. 51–59, Aug 2010.

20. Kor, D. J., C. M. van Buskirk, and O. Gajic, "Red blood cell storage lesion," *Bosnian Journal of Basic Medical Sciences*, Vol. 9, pp. 21–27, Oct 2009.

21. Knutson, F., J. Lööf, and C. F. Högman, "Pre-separation storage of whole blood: the effect of temperature on red cell 2,3-diphosphoglycerate and myeloperoxidase in plasma," *Transfusion Science*, Vol. 21, pp. 111–115, Oct 1999.

22. Zubair, A. C., "Clinical impact of blood storage lesions," *American Journal of Hematology*, Vol. 85, pp. 117–122, Feb 2010.

23. van de Watering, L., "Red cell storage and prognosis," *Vox Sanguinis*, Vol. 100, pp. 36–45, Jan 2011.

24. Chin-Yee, I., N. Arya, and M. S. D'Almeida, "The red cell storage lesion and its implication for transfusion," *Transfusion Science*, Vol. 18, pp. 447–458, Sep 1997.

25. Karon, B. S., C. M. van Buskirk, E. A. Jaben, J. D. Hoyer, and D. D. Thomas, "Temporal sequence of major biochemical events during blood bank storage of packed red blood cells," *Blood Transfusion*, Vol. 10, pp. 453–461, Oct 2012.

26. Grazzini, G., and S. Vaglio, "Red blood cell storage lesion and adverse clinical outcomes: *post hoc ergo propter hoc?*," *Blood Transfusion*, Vol. 10, pp. s4–s6, May 2012.

27. Chaudhary, R., and R. Katharia, "Oxidative injury as contributary factor for red cells storage lesion during twenty eight days of storage," *Blood Transfusion*, Vol. 10, pp. 59–62, Jan 2012.

28. Holme, S., "Current issues related to the quality of stored RBCs," *Transfusion and Apheresis Science*, Vol. 33, pp. 55–61, Aug 2005.

29. Hess, J. R., R. L. Sparrow, P. E. van der Meer, J. P. Acker, R. A. Cardigan, and D. V. Devine, "Red blood cell hemolysis during blood bank storage: Using national quality measurement data to answer basic scientific questions," *Transfusion*, Vol. 49, pp. 2599–2603, Dec 2009.

30. Högman, C. F., and H. T. Meryman, "Red blood cells intended for transfusion: Quality criteria revisited," *Transfusion*, Vol. 46, pp. 137–142, Jan 2006.

31. Makroo, R. N., V. Raina, A. Bhatia, R. Gupta, A. Majid, U. K. Thakur, and N. L. Rosamma, "Evaluation of the red cell hemolysis in packed red cells during processing and storage," *Asian Journal of Transfusion Science*, Vol. 5, pp. 15–17, Jan 2011.

32. Kanias, T., and M. T. Galdwin, "Nitric oxide, hemolysis, and the red blood cell storage lesion: Interaction between transfusion, donor, and recipient," *Transfusion*, Vol. 52, pp. 1388–1392, July 2012.

33. Neal, M. D., J. S. Raval, D. J. Triulzi, and R. L. Simmons, "Innate immune activation after transfusion of stored red blood cells," *Transfusion Medicine Reviews*, Vol. 27, pp. 113–118, Apr 2013.

34. Qazi, M. A., F. G. Rizzatti, B. Piknova, N. Sibmooh, D. F. Stroncek, and A. N. Schechter, "Effect of storae on levels of nitric oxide derivatives in blood componenets," *F1000Research*, Vol. 1, Oct 2012.

35. Novotny, V. M., "Red cell transfusion in medicine: Future challenges," *Transfusion Clinique et Biologique*, Vol. 14, pp. 538–541, Dec 2007.

36. Blasi, B., A. D'Alessandro, N. Ramundo, and L. Zolla, "Red blood cell storage and cell morphology," *Transfusion Medicine*, Vol. 22, pp. 90–96, Apr 2012.

37. Högman, C. F., and H. T. Meryman, "Storage parameters affecting red blood cell survival and function after transfusion," *Transfusion Medicine Reviews*, Vol. 13, pp. 275–296, Oct 1999.

38. Veale, M. F., G. Healey, and R. L. Sparrow, "Effect of additive solutions on red blood cell (RBC) membrane properties of stored RBCs prepared from whole blood held for 24 hours at room temperature," *Transfusion*, Vol. 51, pp. 25S–33S, Jan 2011.

39. Gevi, F., A. D'Alessandro, S. Rinalducci, and L. Zolla, "Alterations of red blood cell metabolome during cold liquid storage of erythrocyte concentrations in CPD-SAGM," *Journal of Proteomics*, Vol. 76, pp. 168–180, Dec 2012.

40. Hess, J. R., "An update on soltions for red cell storage," *Vox Sanguinis*, Vol. 91, pp. 13–19, July 2006.

41. Zimrin, A. B., and J. R. Hess, "Current issues relating to the transfusion of stored red blood cells," *Vox Sanguinis*, Vol. 96, pp. 93–103, Feb 2009.

42. Anniss, A. M., and R. L. Sparrow, "Expression of CD47 (integrin-associated protein) decreases on red blood cells during storage," *Journal of Apheresis Sciences*, Vol. 27, pp. 233–238, Dec 2002.

43. Almac, E., and C. Ince, "The impact of storage on red cell function in blood transfusion," *Best Practice & Research Clinical Anaesthesiology*, Vol. 21, pp. 195–208, June 2007.

44. Sparrow, R. L., G. Healey, K. A. Patton, and M. F. Veale, "Red blood cell age determines the impact of storage and leukocyte burden on cell adhesion molecules, glycophorin A and the release of annexin V," *Transfusion and Apheresis Science*, Vol. 34, pp. 15–23, Feb 2006.

45. Bennett-Guerrero, E., T. H. Veldman, A. Doctor, M. J. Telen, T. L. Ortel, T. S. Reid, M. A. Mulherin, H. Zhu, R. D. Buck, R. M. Califf, and T. J. McMahon, "Evolution of adverse changes in stored RBCs," *Proceddings of the National Academy of Sciences of the United States of America*, Vol. 104, pp. 17063–17068, Oct 2007.

46. Lion, N., D. Crettaz, O. Rubin, and J. D. Tissot, "Stored red blood cells: A changing universe waiting for its map(s)," *Journal of Proteomics*, Vol. 73, pp. 374–385, Jan 2010.

47. Pavenski, K., E. Saidenberg, M. Lavoie, M. Tokessy, and D. R. Branch, "Red blood cell storage lesions and related transfusion issues: A canadian blood services research and development symposium," *Transfusion Medicine Reviews*, Vol. 26, pp. 68–84, Jan 2012.

48. Offner, P. J., "Age of blood: Does it make difference?," *Critical Care*, Vol. 8, pp. s24–s26, June 2004.

49. Aubron, C., A. Nichol, D. J. Cooper, and R. Bellomo, "Age of red blood cells and transfusion in the critically ill patient," *Annals of Intensive Care*, Vol. 3, Jan 2013.

50. Klein, H. G., "How safe is blood, really?," *Biologicals*, Vol. 38, pp. 100–104, Jan 2010.

51. Klein, H. G., D. R. Spahn, and J. L. Carson, "Red blood cell transfusion in clinical practice," *Lancet*, Vol. 370, pp. 415–426, Aug 2007.

52. Lelubre, C., and J.-L. Vincent, "Red blood cell transfusion in the critically ill patient," *Annals of Intensive Care*, Vol. 1, no. 43, 2011.

53. Twomley, K. M., S. V. Rao, and R. C. Becker, "Proinflammatory, immunomodulating, and prothrombotic properties of anemia and red blood cell transfusions," *J Thrombosis Thrombolysis*, Vol. 21, pp. 167–174, Apr 2006.

54. Contreras, M., and M. de Silva, "Acute transfusion reactions," *Bailliere's Clinical Anaesthesiology*, Vol. 11, pp. 205–218, June 1997.

55. Refaai, M. A., and N. Blumberg, "The transfusion dilemma — Weighing the known and newly proposed risks of blood transfusions against the uncertain benefits," *Best Practice & Research Clinical Anaesthesiology*, Vol. 27, pp. 17–35, 2013.

56. Kim-Shapiro, D. B., J. Lee, and M. T. Gladwin, "Storage lesion: Role of red blood cell breakdown," *Transfusion*, Vol. 51, pp. 844–851, Apr 2011.

57. Roback, J. D., "Vascular effects of the red blood cell storage lesion," *Hematology / the Education Program of the American Society of Hematology*, Vol. 2011, pp. 475–479, 2011.

58. Donadee, C., N. J. H. Raat, T. Kanias, J. Tejero, J. S. Lee, E. Kelley, X. Zhao, C. Liu, H. Reynolds, I. Azarov, S. Frizzell, E. M. Meyer, A. D. Donnenberg, L. Qu, D. Triulzi, D. B. Kim-Shapiro, and M. T. Gladwin, "Nitric oxide scavenging by red blood cell microparticles and cell-free hemoglobin as a mechanism for the red cell storage lesion," *Circulation*, Vol. 124, pp. 465–476, July 2011.

59. Tsai, A. G., A. Hofmann, P. Cabrales, and M. Intaglietta, "Perfusion vs. oxygen delivery in transfusion with 'fresh' and 'old' red blood cell: The experimental evidence," *Transfusion and Apheresis Sciences*, Vol. 43, pp. 69–78, Aug 2010.

60. Uvizl, R., B. Klementa, M. Adamus, and J. Neiser, "Biochemical changes in the patient's plasma after red blood cell transfusion," *Signa Vitae*, Vol. 6, no. 2, pp. 64–71, 2011.

61. Doctor, A., and P. Spinella, "Effect of processing and storage on red blood cell function *in vivo*," *Seminars In Perinatology*, Vol. 36, pp. 248–259, Aug 2012.

62. Kleinman, S., P. Chan, and P. Robillard, "Risks associated with transfusion of cellular blood components in Canada," *Transfusion Medicine Reviews*, Vol. 17, pp. 120–162, April 2003.

63. Tinmouth, A., and I. Chin-Yee, "The clinical consequences of the red cell storage lesion," *Transfusion Medicine Reviews*, Vol. 15, pp. 91–107, Apr 2001.

64. Carrillo-Esper, R., C. A. Carrillo-Córdova, J. R. Carrillo-Córdova, and L. D. Carrillo-Córdova, "Storage-induced morphological changes in erythrocytes," *Rev Invest Med Sur Mex*, Vol. 19, no. 1, pp. 10–14, 2012.

65. Barshtein, G., N. Manny, and S. Yedgar, "Circulatory risk in the transfusion of red blood cells with impaired flow properties induced by storage," *Transfusion Medicine Reviews*, Vol. 25, pp. 24–35, Jan 2011.

66. Keidan, I., G. Amir, M. Mandel, and D. Mishali, "The metabolic effects of fresh versus old stored blood in the priming of cardiopulmonary bypass solution for pediatric patients," *The Journal of Thoracic and Cardiovascular Surgery*, Vol. 127, pp. 949–952, Apr 2004.

67. Greenwalt, T. J., "A short history of transfusion medicine," *Transfusion*, Vol. 37, pp. 550–563, May 1997.

68. Solheim, B. G., O. Flesland, J. Seghatchian, and F. Brosstad, "Clinical implications of red blood cell and platelet storage lesions: An overview," *Transfusion and Apheresis Science*, Vol. 31, pp. 185–189, Dec 2004.

69. Schuetz, A. N., K. L. Hillyer, J. D. Roback, and C. D. Hillyer, "Leukoreduction filtration of blood with sickle cell trait," *Transfusion Medicine Reviews*, Vol. 18, pp. 168–176, July 2004.

70. Burger, P., H. Korsten, A. J. Verhoeven, D. de Korte, and R. van Bruggen, "Collection and storage of red blood cells with anticoagulant and additive solution with a physiologic pH," *Transfusion*, Vol. 52, pp. 1245–1252, June 2012.

71. BCSH Blood Transfusion Task Force, "Guidelines on gamma irradiation of blood components for the prevention of transfusion-associated graft-versus-host disease," *Transfusion Medicine*, Vol. 6, pp. 261–271, Sep 1996.

72. Yoshida, T., J. P. AuBuchon, L. Tryzelaar, K. Y. Foster, and M. W. Bitensky, "Extended storage of red blood cells under anaerobic conditions," *Vox Sanguinis*, Vol. 92, pp. 22–31, Jan 2007.

73. Llohn, A. H., A. Vetlesen, M. K. Fagerhol, and J. Kjeldsen-Kragh, "The effect of pre-storage cooling on 2,3-DPG levels in red cells stored in SAG-M," *Transfusion and Apheresis Sciences*, Vol. 33, pp. 113–118, Oct 2005.

74. Purdy, F. R., M. G. Tweeddale, and P. M. Merrick, "Association of mortality with age of blood transfused in septic ICU patients," *Canadian Journal of Anaesthesia*, Vol. 44, pp. 1256–1261, Dec 1997.

75. Yuruk, K., R. Bezemer, and C. Ince, "The ability of red blood cell transfusions to reach the microcirculation," *Annual Update in Intensive Care and Emergency Medicine*, Vol. 2012, pp. 431–440, 2012.

76. Selim, N. S., O. S. Desouky, E. M. Elbakrawy, and R. A. Rezk, "Electrical behavior of stored erythrocytes after exposure to gamma radiation and the role of α-lipoic acid as radioprotector," *Applied Radiation and Isotopes*, Vol. 68, pp. 1018–1024, June 2010.

77. Harmening, D. M., *Modern Blood Banking and Transfusion Practices*, Philadelphia: F. A. Davis Company, 6^{th} ed., 2012.

78. Zehnder, L., T. Schulzki, J. S. Goede, J. Hayes, and W. H. Reinhart, "Erythrocyte storage in hypertonic (SAGM) or isotonic (PAGGSM) conservation medium: Influence on cell properties," *Vox Sanguinis*, Vol. 95, pp. 280–287, Nov 2008.

79. Mintz, P. D., and G. Anderson, "Effect of gamma irradiation on the *in vivo* recovery of stored red blood cells," *Annals of Clinical and Laboratory Science*, Vol. 23, no. 3, pp. 216–220, 1993.

80. Glynn, S. A., "The red blood cell storage lesion: A method to madness," *Transfusion*, Vol. 50, pp. 1164–1169, June 2010.

81. Zhao, T. X., and A. Shanwell, "Electrical impedance alterations of red blood cells during strorage," *Vox Sanguinis*, Vol. 66, no. 4, pp. 258–263, 1994.

82. Ülgen, Y., and M. Sezdi, "Physiological quality assessment of stored whole blood by means of electrical measurements," *Medical & Biological Engineering & Computing*, Vol. 45, pp. 653–660, July 2007.

83. Sezdi, M., *Modeling of Physiological Properties of Stored Human Blood by Complex Impedance Measurements*. PhD thesis, Bogazici University, Istanbul, Turkey, 2005.

84. Sezdi, M., M. Bayik, and Y. Ülgen, "Strorage effects on the Cole-Cole parameters of erythrocyte suspensions," *Physiological Measurement*, Vol. 27, pp. 623–635, July 2006.

85. Lim, H. J., J. H. Nam, B. K. Lee, J. S. Suh, and S. Shin, "Alteration of red blood cell aggregation during blood storage," *Korea-Australia Rheology Journal*, Vol. 23, pp. 67–70, June 2011.

86. Acker, J. P., I. M. Croteau, and Q. L. Yi, "An analysis of the bias in red blood cell hemolysis measurement using several analytical approaches," *Clinica Chimica Acta*, Vol. 413, pp. 1746–1752, Nov 2012.

87. Meinke, M., M. Friebel, J. Helfmann, and M. Notter, "A novel device for non-invasive measurement of free hemoglobin in blood bags," *Biomedizinische Technik*, Vol. 50, no. 1-2, pp. 2–7, 2005.

88. Wyszecki, G., and W. S. Stiles, *Color Science: Concepts and Methods, Quantitative Data and Formulae*, New York: John Wiley & Sons, 2^{nd} ed., 2000.

89. "The physiology of human vision," tech. rep., Adobe System Inc., 2000.

90. Marieb, E. N., J. Mallatt, and P. B. Wilhelm, *Human Anatomy*, San Francisco: Pearson/Benjamin Cummings, 6^{th} ed., 2005.

91. "Recommended system for mesopic photometry based on visual performance," tech. rep., Lighting Analysts Inc., Vienna, Austria, 2010.

92. Purkinje, J., "Beobachtungen und versuch zur physiologie der sinne," *Zweites BÃndchen: Neue BeitrÃge zur Kenntnis des Sehens in subjektiver Hinsicht*, Vol. 192, pp. –, 1825.

93. Newton, I., "A new theory about light and colors," *Philosophical Transactions of the Royal Society VI*, Vol. 80, pp. 3075–3087, Feb 1672.

94. Grassmann, H. G., "On the theory of compound colors," *Philosophical Magazine S.4*, Vol. 7, pp. 254–264, Apr 1854.

95. Maxwell, J. C., "On the theory of compound colours, and the relations of colour of the spectrum," *Philosophical Transactions of the Royal Society of London*, Vol. 150, no. 1, pp. 57–84, 1860.

96. Bouma, P. J., *Physical Aspects of Colour: An Introduction to the Scientific Study of Colour Stimuli and Colour Sensations*, New York: St. Martin's Press Inc, 1971.

97. Munsell, A. H., *A Color Notation*, Boston: Ellis, 1905.

98. Ostwald, W., *The Color Primer; a basic treatise on the color system of Wilhelm Ostwald*, New York: Van Nostrand Reinhold, 1969.

99. "International lighting vocabulary," tech. rep., Commision Internationale de l'Eclairage, 1987.

100. Evans, R. M., *An Introduction to Color*, New York: John Wiley & Sons, 1948.

101. Guild, J., "The colorimetric properties of the spectrum," *Philosophical Transactions of the Royal Society of London A*, Vol. 230, pp. 149–187, 1931.

102. Wright, W. D., "A re-determination of the trichromatic coefficients of the spectral colours," *Transactions of the Optical Society*, Vol. 30, no. 4, pp. 141–164, 1929.

103. "Commision internationale de l'eclairage proceedings," tech. rep., CIE, Cambridge, 1931.

104. Hunt, R. W. G., *Measuring Color*, London: Ellis Horwood, 2^{nd} ed., 1991.

105. "Colorimetry, official recommendations of the cie," tech. rep., Commision Internationale de l'Eclairage, Paris, 1971.

106. Hunter, R. S., *Photoelectric tristimulus colorimetry with three filters circular*, Washington: National Bureau of Standards, 1942.

107. "Color models: CIELuv," tech. rep., Adobe System Inc., 2000.

108. Westland, S., *Computational Color Science Using Matlab*, Chichester: J. Wiley & Sons, 2012.

109. Sharp, J., "Coated printed circuit board reflectance with the R400-7-VIS-NIR reflection probe," tech. rep., Ocean Optics, July 2006.

110. Han, V., K. Serrano, and D. V. Devine, "A comparative study of common techniques used to measure haemolysis in stored red cell concentrates," *Vox Sanguinis*, Vol. 98, pp. 116–123, Feb 2010.

111. Blakney, G. B., and A. J. Dinwoodie, "A spectrophotometric scanning technique for the rapid determination of plasma hemoglobin," *Clinical Biochemistry*, Vol. 8, pp. 96–102, Apr 1975.

112. Leon, K., D. Mery, F. Pedreschi, and J. León, "Color measurement in L*a*b* units from RGB digital images," *Food Research International*, Vol. 39, no. 10, pp. 1084–1091, 2006.

113. Balas, C., "An imaging colorimeter for noncontact tissue color mapping," *IEEE Transactions on Biomedical Engineering*, Vol. 44, pp. 468–474, June 1997.

114. Marszalec, E., and M. Pietikäinen, "Color measurements based on a color camera," *Proceedings SPIE*, Vol. 3101, pp. 170–181, June 1997.

115. Chandran, J., A. Stojcevski, A. Zayegh, and T. Nguyen, "Implementation of a colorimetric algorithim for portable blood gas analysis," *22th International Conference on Microelectronics*, 2010.

116. Overheim, R. D., and D. L. Wagner, *Light and Color*, New York: John Wiley & Sons, 1^{st} ed., 1982.

117. Vandromme, M. J., G. J. McGwin, and J. A. Weinberg, "Blood transfusion in the critically ill: does storage age matter?," *Scandinavian Journal of Trauma, Resuscitation and Emergency Medicine*, Vol. 17, Aug 2009.

118. Leitner, G. C., P. Jilma-Stohlawetz, G. Stiegler, G. Weigel, M. Horvath, A. Tanzmann, P. Höcker, and M. B. Fisher, "Quality of packed red blood cells and platelet concantrates collected by multi-component collection using the mcs plus device," *Journal of Clinical Apheresis*, Vol. 18, no. 1, pp. 21–25, 2003.